CRYSTAL GROWTH & DESIGN

pubs.acs.org/crystal

Perspective

Advances in Low-Frequency Vibrational Spectroscopy and Applications in Crystal Engineering

Elyse M. Kleist and Michael T. Ruggiero*

Cite This: *Cryst. Growth Des.* 2022, 22, 939−953

Read Online

ACCESS | Metrics & More | Article Recommendations

ABSTRACT: The field of low-frequency vibrational spectroscopy has grown significantly over the past two decades, based on advances in both experimental lasers and optics, as well as high-performance computing and quantum mechanical simulations. The combination of these techniques has enabled unprecedented insight into the atomic-level dynamics that occur at terahertz frequencies, which usually involve large-amplitude motions of entire molecules. This has ultimately provided the community with new tools for investigating and engineering crystalline materials through an understanding of intermolecular forces, as well as dynamics. In this Perspective, an overview of the field will be provided and complemented by recent examples where low-frequency vibrational motions are being used to understand, and drive, bulk material function.

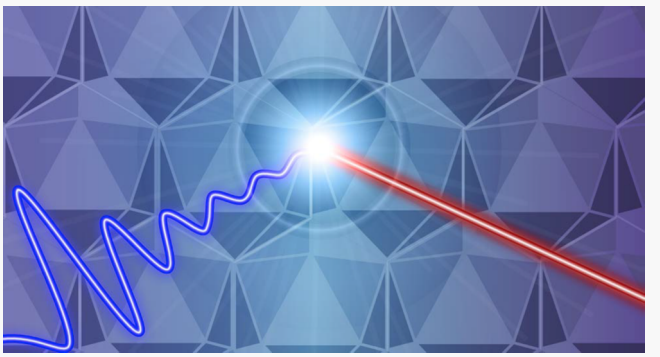

INTRODUCTION

Over the last three decades, the field of low-frequency (terahertz) vibrational spectroscopy has evolved from humble beginnings as a boutique method, often performed at large-scale synchrotron or free-electron laser facilities, to current state-of-the-art technologies where multiple manufacturers are producing benchtop instruments costing less than $100,000.[1−3] This has resulted in an explosion of new users, spanning a range of disciplines, including condensed matter physics,[4,5] chemical engineering,[6] biotechnology,[7−9] and even the heritage and archival sciences.[10−13] The rapid growth of the terahertz sciences has resulted in a barrage of new applications, as the increasing understanding of terahertz dynamics is unlocking countless new research directions, particularly for crystalline solids.[14,15]

Low-frequency vibrational spectroscopy, covering a spectral range loosely defined from 0.3 to 10 THz or 10 to 333 cm^{-1}, generally involves the excitation of vibrations that often exhibit large-amplitude intermolecular motions, in many cases involving entire molecules. This makes terahertz spectroscopy an effective probe of the entire potential energy hypersurface, resulting in the ability to describe phenomena that are fundamentally linked to weak noncovalent forces. One of the earliest and continued applications of terahertz spectroscopy is in the identification of crystalline polymorphs, as the strong dependence of low-frequency dynamics on the intermolecular coordinate results in each unique bulk structure exhibiting its own spectral fingerprint at terahertz frequencies.[16−18] Yet, despite this obvious utility, the dependence of terahertz dynamics on intermolecular forces is also the technique's "Achilles' Heel". Unlike more traditional mid-infrared (mid-IR) spectroscopies, functional group-specific transitions at terahertz frequencies do not exist, making the analysis of low-frequency vibrational spectroscopy data near-impossible for systems containing more than a few atoms without additional insight. Over the last two decades, advances in high-performance computing, coupled with the development of robust periodic density functional theory (DFT) software packages, have remedied this, with the ability to simulate terahertz vibrational spectra (along with vibrational motions) now common in most modern software packages. When coupled, experimental low-frequency vibrational spectroscopy and quantum mechanical simulations provide a powerful data set that can be used to understand the fundamental forces in crystalline materials, which ultimately dictate the atomic and bulk properties of materials—all with atomic-level insight.

Over the years, the advantages of obtaining high-quality terahertz vibrational spectra, along with the simultaneous interpretation of the data using periodic DFT simulations, have become increasingly apparent.[19] After early studies on the

Received: July 27, 2021
Revised: September 21, 2021
Published: October 15, 2021

https://doi.org/10.1021/acs.cgd.1c00850
Cryst. Growth Des. 2022, 22, 939−953

identification and characterization of crystalline polymorphs using low-frequency vibrational spectroscopy, the field grew, making use of insight gained through the binary experimental and computational approach to understand the subtle origins of polymorph stability, in many cases pinpointing the exact interaction(s) that are responsible for the preference of one crystalline form over another—with some examples involving differences in energies of less than a kJ mol^{-1}.[20,21] While not inherently a structural technique, the terahertz community learned to leverage the dependence of terahertz spectroscopy on weak intermolecular forces to uncover incredibly subtle differences in the structures and interactions found in crystals that have similar, and in some cases nearly identical, structures, where it has been shown that terahertz data can provide details that are not captured by X-ray diffraction (XRD) methods. In turn, the coupling of low-frequency vibrational spectroscopy, XRD, and *ab initio* simulations has yielded one of the most powerful combinations of techniques for investigating crystalline structure and dynamics, and together these techniques form the basis for new research thrusts into the field of crystal structure prediction—with the terahertz analyses often providing critical insight into overcoming ambiguous diffraction results.

As the field has evolved, the community has learned to leverage the actual terahertz vibrational motions themselves to understand material properties from a new perspective. Some of the first examples in this respect were the discoveries in which many solid-state phase transformation processes follow a mechanism that is often correlated to a single low-frequency vibrational mode.[22,23] Even adsorption of gas molecules by porous organic crystals has been suggested to be dictated by terahertz dynamics.[24,25] Over the years, the intimate link between solid-state phase transitions and terahertz normal modes has been validated numerous times, and it is now becoming common practice not only to characterize phase transitions using low-frequency vibrational spectroscopy but also to promote such processes using terahertz radiation alone—demonstrated for example in polymers,[26] disordered solids,[27] and inorganic crystals.[28] This area of the terahertz sciences is highly active and represents some of the most cutting-edge work currently being performed.[29,30]

In addition, over the past decade as the community has learned more about the role that THz dynamics play on material functions ranging from sub-nanometer to bulk phenomena, a number of creative applications have resulted. One recent example was the discovery that electron−phonon coupling in organic semiconducting crystals is dominated by a single terahertz phonon mode, which has provided unprecedented insight into a process that was previously difficult to understand and has opened up a new research field into "phonon engineering" to design more effective semiconducting materials.[31,32] Another example, an entirely new area of research involving the determination of the mechanical response of solids using low-frequency vibrational spectroscopy, has grown over the past decade due to the dependence of both elastic constants and terahertz dynamics on intermolecular forces. This has resulted in methods for extracting bulk elastic information from experimental terahertz spectra, as well as new computational tools for decomposing the elastic constants into contributions from individual vibrational normal modes.[33] As the field has grown, insights into the mechanical response of biomolecular crystals,[34] porous frameworks,[35] and organic semiconductors[36] have all been uncovered.

Overall, the terahertz sciences have exploded in popularity over the past few decades, and the efforts of the small, but active and growing, community have laid the foundation for exciting new directions that link molecular and bulk structures, dynamics, and properties. In this Perspective, a historical account of the major developments in the terahertz and low-frequency Raman (LFR) fields is discussed, followed by a description of the origins of terahertz vibrations in solids. Subsequently, the applications of low-frequency vibrational spectroscopy to the study of crystalline polymorphs are reviewed, including more recent applications for studying solid-state phase transitions, including state-of-the-art applications in driving phase transitions using terahertz radiation alone. Finally, the cutting-edge application of low-frequency spectroscopy to determine the mechanical response of materials is highlighted, and future directions are addressed.

TECHNIQUES

Terahertz Spectroscopy. Historically, there has been considerable difficulty in generating and detecting terahertz-frequency electromagnetic radiation, as it is too high in frequency to detect and generate electronically and too low in energy to be detected by semiconductors. While previously referred to as the "terahertz gap", the field of far-infrared spectroscopy accessed this region prior to the mid-20th century, but investigations were limited to techniques that employed incoherent light sources, including the extension of Fourier-transform infrared spectroscopy (FTIR) to the terahertz region, or synchrotron/free-electron laser sources.[2,37] Many of these studies used helium-cooled bolometers as detectors, which, while expensive to operate, are very sensitive and continue to be used today.[38,39]

Surprisingly, modern terahertz spectroscopy did not grow from the FTIR community; rather, it emerged from work in electrical engineering, originating from the pursuit of detecting ultrafast electrical signals—beginning with the utilization of picosecond gratings in semiconductor devices to control electronic switches with ultrafast picosecond optical pulses in 1975 by Auston et al.[40,41] Although this was not the original intention, these switches functioned as photoconductive transmitters and detectors, which led to the eventual generation and detection of terahertz pulses.[42−44] As shown in Figure 1, these photoconductive antennae (PCA) operate by applying a bias voltage to a metal dipole antenna patterned on a photoconductive substrate. At the same time, ultrafast optical pulses are focused onto the antenna and generate free carriers

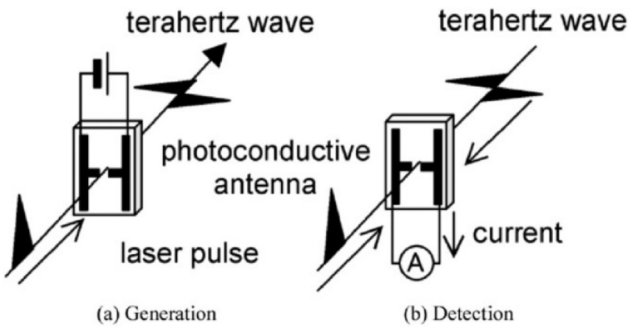

Figure 1. Schematic of (a) generation and (b) detection of terahertz radiation with PCA. Reprinted with permission from ref 49. Copyright 2013 Wiley.

https://doi.org/10.1021/acs.cgd.1c00850
Cryst. Growth Des. 2022, 22, 939−953

that are accelerated by the bias voltage to produce a transient photocurrent that ultimately radiates terahertz pulses. A similar process is employed for detection, except without a bias voltage applied to the dipole antenna receiver, and instead, the terahertz pulse induces a transient bias. An optical pulse is then used to generate photocarriers, where the measured generated current is proportional to the incident terahertz field strength. The delay time between the terahertz and optical pulses allows for direct measurement of the entire terahertz electric field, which can be used to directly obtain the complex dielectric function.[45−48]

In parallel to work on PCA in the late-20th century, the development of nonlinear crystals for electro-optic generation and sampling[50−53] was first demonstrated for femtosecond electrical transients,[54] then for detection of free-space transients.[55] From this pioneering work, the field of terahertz sciences flourished, producing new ways to generate and detect terahertz radiation in traditional academic laboratories.[2,56−60] These advances, coupled with improvements in ultrafast laser technology, fueled the commercialization of affordable benchtop spectrometers and increased the accessibility of terahertz spectroscopy.[48,60,61]

Low-Frequency Raman Spectroscopy. Unlike terahertz spectroscopy, which is fundamentally an absorption method, Raman spectroscopy measures the inelastic scattering of light to probe molecular motions.[62,63] Although the majority of the signal comes from elastic scattering (i.e., Rayleigh scattering), Raman scattering occurs through inelastic processes where incident photons scatter with lower or higher energy than the excitation source (Stokes and anti-Stokes scattering, respectively), with the energy difference between the incident photon and the scattered photon corresponding to the energy difference between vibrational states.[64,65]

In Raman spectroscopy, the wavelengths of Stokes and anti-Stokes scattering signals ($\lambda_{\text{scattered}}$) are relative to the incident excitation wavelength ($\lambda_{\text{incident}}$) and generally are reported as a Raman shift in wavenumbers ($\Delta\tilde{\nu}$ as shown in eq 1, which ultimately enables direct comparison between experiments utilizing different excitation sources.

$$\Delta\tilde{\nu} = \left(\frac{1}{\lambda_{\text{incident}}} + \frac{1}{\lambda_{\text{scattered}}}\right) \tag{1}$$

While traditional mid-IR Raman spectroscopy has been a powerful analytical tool for much of the past decade, LFR spectroscopy, which corresponds to Raman shifts in the terahertz region, is much less common. This is primarily due to the proximity of the terahertz region to the Rayleigh peak, which requires very tight rejection-wavelength tolerances. For example, according to eq 1, when using a 532 nm excitation wavelength, Raman Stokes shifts in the terahertz region (0.3−3 THz) occur between 531.7 and 529.2 nm, while excitation with 785 nm corresponds to shifts from 784.4 to 778.9 nm.

Notch or edge filters used in traditional Raman instruments are suitable for accessing the mid-IR spectral region since the Raman shift is hundreds to thousands of wavenumbers away from the Rayleigh peak. Although both types of filters effectively block the Rayleigh peak with rejection bandwidths on the order of hundreds of wavenumbers, in doing so, they block most, if not all, of the terahertz region. Revealing useful signals in the terahertz region has been possible with several approaches, such as triple grating spectrometers, near excitation tunable filter accessories, and multiple edge filters, but the focus here is on the advances in notch filter technology to properly attenuate the strong Rayleigh peak.[66,67] Ultranarrow bandwidth notch filters, with rejection bandwidths <10 cm^{-1} rather than hundreds of wavenumbers like traditional notch filters, employ volume holographic gratings (VGHs) to block only the wavelength of the excitation laser while transmitting Raman signals.[68,69]

In addition, the efficacy of ultranarrow filters in suppressing Rayleigh scattering relies on matching the incoming laser frequency to the particular filter, which influences the rejection bandwidth. Standard diode lasers often emit multiple wavelengths and can increase the background noise of a measurement through amplified spontaneous emission (ASE). Wavelength-stable diode lasers coupled with matching VGH notch and ASE suppression filters have made it possible to access and collect low-frequency spectra with commercially available instruments. Accessibility of LFR spectrometers has grown with these significant improvements in filters and diode lasers, leading to a number of commercial instruments that are affordable, while boasting rapid measurement times.[61,67,70] It is important to note that, for Raman measurements, the detection method is not as complex as in terahertz spectroscopy, as the detected radiation most often occurs in the visible region of the electromagnetic spectrum where multiple detector types are sufficient, and highly sensitive spectrometers are readily available.[67,69]

Character of Low-Frequency Modes. All chemical vibrational phenomena are governed by the same set of conditions and are commonly described by the solution to the harmonic oscillator Schrödinger equation,

$$E_\nu = \nu + \frac{1}{2}\hbar\sqrt{\frac{k}{\mu}} \tag{2}$$

where E_ν is the energy of the νth-vibrational level, $\hbar$ is the reduced Planck's constant, k is the vibrational force constant, and μ is the reduced mass of the oscillator. Mid-IR vibrations involve localized, intramolecular motions, whose force constants are often dictated by the strengths of the covalent bonds involved in the motions. This can be inferred from eq 2, where a vibration involving a covalent bond would have a large force constant (k) and thus a large transition frequency. While covalent bond strengths can certainly vary between different molecules/structures, such variations are rather limited in magnitude, giving rise to the characteristic functional group frequencies in the mid-IR.[71] On the other hand, low-frequency vibrations in crystalline materials are dominated by intermolecular interactions, which typically have small force constants as well as large reduced masses and can differ considerably based on a large number of factors, including the molecular conformation, the identity and conformations of surrounding molecules, bulking packing structure, and so on. Figure 2 illustrates the difference between intramolecular and intermolecular motions with a comparison of the bending vibration for a single molecule of carbon disulfide and the hindered-rotational lattice vibration for crystalline carbon disulfide.[72] From eq 2, these low-frequency vibrations originate from either small force constants or large reduced masses; conditions that are satisfied in crystals when weak intermolecular forces are involved and when many atoms are in motion.

With the discussion of the origins of the spectral features found in the mid-IR and terahertz regions, the infrared/Raman

https://doi.org/10.1021/acs.cgd.1c00850
Cryst. Growth Des. 2022, 22, 939−953

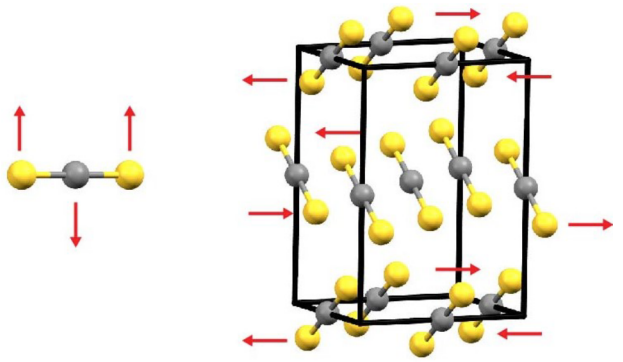

Figure 2. Example of intramolecular bending vibration in a single carbon disulfide molecule (left) and intermolecular hindered-rotation motion in crystalline carbon disulfide (right).

activity of a vibration must also be addressed. In the mid-IR, a vibration will be infrared-active if, over the course of the vibration, there is a change in the dipole moment of a molecule, and Raman-active if there is a change in polarizability.[64] These rules extend to the low-frequency vibrations of crystalline materials, but instead of a change in the dipole moment or polarizability of a molecule, the change must occur over the crystalline unit cell.[73]

Computational Methods. The ability of low-frequency vibrational spectroscopy to probe weak intermolecular forces and excite large-amplitude vibrations is at the core of its utility. Specifically advanced computational models, often based on DFT simulations, have proven to be the "gold-standard" for the assignment of experimental low-frequency vibrational data for crystals containing more than a few atoms.[74]

Because of the exceptionally weak forces that drive low-frequency vibrational dynamics, it is crucial that simulation methods provide highly accurate and numerically robust descriptions of the electronic structure and associated values (i.e., interatomic forces), in order to effectively be used for understanding experimental data.[75] Over the last two decades, major strides in the field of computational vibrational spectroscopy of solids have been made, moving the field from originally being unable to study crystalline vibrational dynamics accurately, to its current state, where simulations on large and complex solids can be performed with relative ease. Some pioneering work involved the realization that gas-phase simulations were not appropriate for reproducing crystalline terahertz dynamics,[16,76−78] the implementation of vibrational analyses in periodic DFT software packages,[79,80] the inclusion of London dispersion corrections into the DFT framework,[81−88] and, in parallel to these algorithmic developments, the rapid increase in high-performance computing technology. Additionally, while most mid-IR vibrations can be accurately modeled within the harmonic approximation (see eq 2), terahertz vibrations are often highly excited—even at low temperatures—and thus anharmonic effects must often be considered to accurately describe low-frequency vibrations. Recently, a number of anharmonic vibrational methods have been implemented in DFT software packages, and they have been applied in various capacities to help describe the terahertz dynamics of crystalline and disordered solids.[20,89−92]

Over the years, numerous DFT software packages have been released that enable the inclusion of periodic boundary conditions, with most still being actively developed. The most significant difference between these packages involves the underlying model for reproducing the atomic wave functions, basing them on atomic-centered Gaussian-type orbitals (CRYSTAL[93]), plane waves (VASP,[94] Quantum ESPRESSO,[95,96] DMol3[97]), or a combination of the two (CP2K[98,99]). While the different codes might be tailored to different material types, for example, atom-centered basis sets more readily enable chemical insight and are well-suited for molecular crystals,[100,101] while plane-wave codes are usually better for inorganic solids and conductors; ultimately, all of these software packages are capable of accurately simulating the low-frequency vibrational dynamics of crystalline solids.

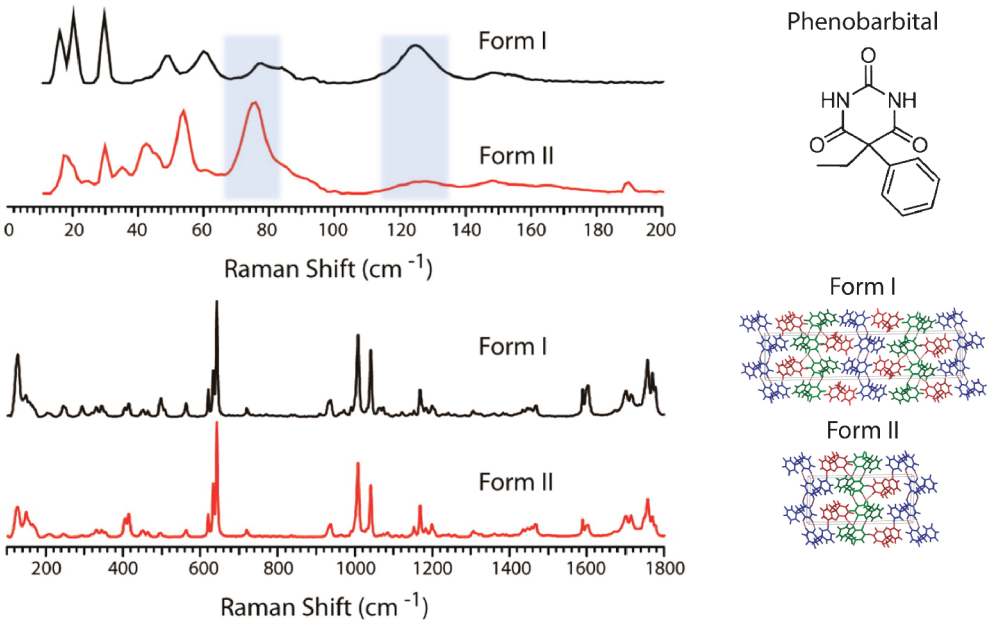

Figure 3. LFR spectra of polycrystalline phenobarbital and crystal structures of polymorphic Forms I and II. Image adapted with permission from ref 18. Copyright 2013 American Chemical Society.

https://doi.org/10.1021/acs.cgd.1c00850
Cryst. Growth Des. 2022, 22, 939−953

This has resulted in users having more choice than ever in this regard, which is apparent in the current literature.[102−110]

APPLICATIONS IN CRYSTALLINE SYSTEMS

Characterization of Crystal Structures and Associated Properties. The relationship between low-frequency vibrations and weak, often intermolecular, forces results in a strong dependence of terahertz and LFR spectra on the solid-state structures of materials, making them excellent tools for investigating polymorphism. While mid-IR transition frequencies can certainly vary between polymorphs, such differences are constrained to a narrow range due to the relatively constant covalent bond force constants. On the other hand, various factors influence intermolecular forces in solid materials, including molecular structure, immediate neighbors, and in many cases, long-range contacts that can extend over a few nanometers. Thus, any change in the bulk geometry of condensed phase materials, corresponding to a change in the intermolecular forces, would dramatically affect the low-frequency vibrational spectra.

While terahertz and Raman spectroscopies do not directly measure structural information, they are an indirect probe due to the strong dependence of terahertz and LFR spectra on bulk structure. In this sense, low-frequency vibrational spectroscopies are advantageous compared to common structural methods, such as XRD, because they can help elucidate the structures of materials whose diffraction data might be ambiguous.[111,112] In this respect, pioneering work of the early 2000s grew from the study of pharmaceutical polymorphs. After the unfortunate case of ritonavir, where a solid-state phase transition to a previously unknown polymorphic form rendered the drug useless, the pharmaceutical industry has committed itself to understand, predict, and uncover polymorphs of active pharmaceutical ingredients (APIs).[17,113] Early applications of low-frequency spectroscopy focused on polymorphs of well-known APIs, including carbamazepine,[114] ranitidine hydrochloride,[115] indomethacin,[116] sulfathiazole,[117] caffeine,[118] and many others.[61,119−121]

The utility of LFR for differentiating between polymorphs is highlighted in Figure 3 for the anticonvulsant phenobarbital. In crystalline phenobarbital, there are two nearly identical polymorphic forms with only very subtle differences in the packing, which result in Form II having a doubled crystallographic *b*-axis compared to Form I.[18] While the two similar structures can be effectively differentiated using single-crystal XRD, they are indiscernible when using powder XRD. A comparison between the far- and mid-IR behavior of phenobarbital is shown in Figure 3. The mid-IR Raman shifts for both phenobarbital polymorphs are nearly identical; yet, the subtle structural differences are sufficient to alter the intermolecular potential energy landscape, resulting in two different LFR spectra.

Chemometric analysis of mixtures with low-frequency vibrational techniques was demonstrated to be comparably effective to more traditional techniques, including mid-IR spectroscopy and diffraction methods. However, the strong sensitivity of low-frequency vibrational spectra to the bulk packing arrangement makes the terahertz region more attractive for chemometric studies of polymorphic systems, where mid-IR data would likely be ambiguous. Although the first applications were in mixtures of polymorphic APIs,[122,123] and even in determining the amount of crystalline content in bulk samples,[124,125] recent applications have spanned a wide range of materials including binary mixtures of visually similar pigments,[126] ternary mixtures of polymorphs of piroxicam,[127] mixtures of crystalline amino acids,[128] and the quantification of cocrystal species.[129]

While these examples showcased the ability to discern between different polymorphs with low-frequency vibrational spectroscopy, they did not offer a means for interpretation of the experimental spectra. Supplementing experimental spectra with quantum mechanical simulations provides a detailed description of the low-frequency vibrations, including mode-types, frequencies, and intensities.[74] Critically, the combination of experimental low-frequency vibrational spectroscopy and accurate DFT simulations provides a powerful data set that firmly supports the use of such a binary approach to the study of crystalline materials. The first successful demonstrations of this powerful combination were carried out on carbamazepine,[16] ephedrine,[130] octogen,[131] and hydrogen-bonded systems.[132−135] Following these early demonstrations, the utility of this approach was apparent and led to applications spanning biologically relevant molecules,[102,103,110,136] illicit drugs,[137−140] pharmaceuticals,[8,141−143] explosives,[144−146] and pigments.[147,148]

Specifically, because of the dependence of terahertz vibrations on some of the weakest intermolecular forces found in crystals, the successful reproduction of low-frequency vibrational spectra implies that the forces—not only the weak forces but, by extension, all forces—are well-modeled, lending significant confidence to the theoretical model. This can be illustrated with an OH bond, wherein if the interactions of that bond are incorrectly modeled, then subsequently all related forces will likely be flawed, ultimately yielding a poor terahertz spectral simulation. However, if the predicted low-frequency vibrational spectra are well reproduced, then not only are the intermolecular forces well modeled but, also, the covalent forces as well.

This, in turn, enables a deeper understanding of related phenomena without the need for further experimentation. For example, the direct dependence of thermodynamic parameters on the vibrational energy levels implies that accurate reproduction of the low-frequency vibrational spectrum results in an equally accurate determination of thermodynamic values such as entropy and Gibbs/Helmholtz energies. This facet of the binary approach has been leveraged to uncover the stabilities of polymorphs on countless occasions, with a high degree of success.[149−153]

An example of this binary approach was used to understand the thermodynamics surrounding the temperature- and pressure-induced phase transformation between an ordered and orientationally disordered phase of camphor.[20] In this work, temperature- and pressure-dependent terahertz spectroscopy measurements were used to characterize the phase transformation, which was readily achieved due to the dramatic change in the experimental spectra between the two phases. When coupled to *ab initio* molecular dynamics and DFT simulations, the low-frequency vibrational spectroscopy data were used to help uncover the structure of the orientationally disordered phase, which was previously unknown, as well as the mechanism of the transition. The structure for the HT phase was used as the basis for the thermodynamic evaluation. Using static harmonic, as well as quasiharmonic (QHA), DFT simulations, the thermodynamic parameters for the two phases were determined, and the points at which the phase transition occur were predicted based on the temperatures and pressures

https://doi.org/10.1021/acs.cgd.1c00850
Cryst. Growth Des. 2022, 22, 939−953

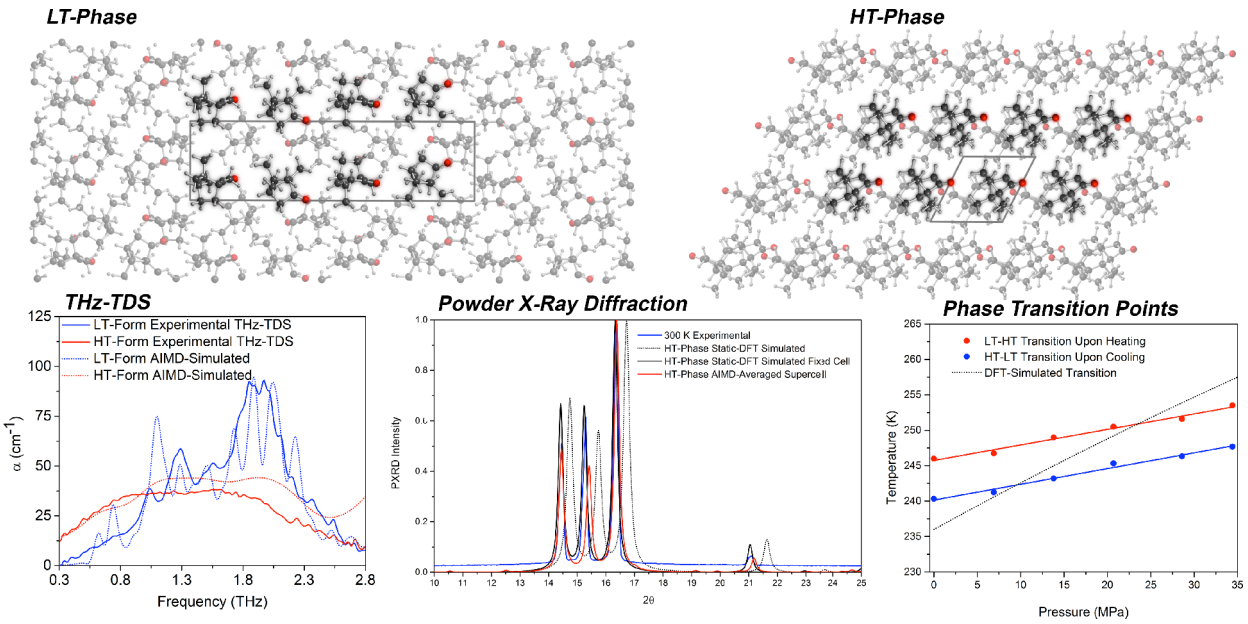

Figure 4. Comparison between the perfectly ordered low-temperature experimental structure (LT phase) and the orientationally disordered high-temperature (HT phase) of the molecular solid camphor. The structure of the HT phase was uncovered using experimental terahertz spectroscopy and AIMD simulations with the predicted and experimental powder XRD data, as shown. The vibrational results were used to predict the temperatures and pressures at which the energetic ordering between the two forms flips, which was shown to be in agreement with experimental data. Reproduced from ref 20. Copyright 2018 American Physical Society.

at which one phase became more stable than the other. The results, shown in Figure 4, highlight that there was an excellent agreement between experiment and theory. This insight was then used to predict the energy barrier for the transformation and calculations using the Arrhenius theory produced a frequency factor that was in excellent agreement with the experimentally observed vibrational frequency for the mode that mapped out the phase change mechanism.

Phase Transformation. Understanding the thermodynamic driving forces can yield useful information involving the stability of crystalline forms but on its own does not provide insight into the mechanisms behind solid-state transformations, including recrystallization of amorphous materials to crystalline, amorphization of crystalline to amorphous, solvation or desolvation, and polymorphic transformations, all of which can be influenced by external forces such as temperature, pressure, and humidity.[154,155] Understanding these transformations is especially useful in solid pharmaceuticals, where these changes can impact the bioavailability and stability of APIs, as well as in other applications such as semiconductors where changes in crystal packing can strongly affect the electrical properties of the materials.[156,157]

As mentioned in the previous section, low-frequency vibrational spectroscopy has been used to identify and quantify polymorphs because of the sensitivity of low-frequency motions to long-range order and changes in the intermolecular forces and thus the structure and energy of a system. However, at its core, low-frequency vibrational methods are dynamic methods, meaning that they are probing quantized vibrational motions—motions that, in the terahertz region, involve large-amplitude displacements of entire molecules. These properties directly lend themselves to characterizing the mechanisms of solid-state phase transformation processes. Investigations of such dynamical transitions have historically been limited, as XRD data only provide an averaged (and effectively static) view of atomic dynamics. Recently, the connections between low-frequency dynamics and phase transformations have been established, making low-frequency spectroscopies ideal tools for characterizing these solid-state changes.[20]

Early investigations into solid-state transformations mainly focused on polymorphic changes that could be controlled externally via temperature. Zeitler et al. explored the kinetics of the transformation between Forms I and III of carbamazepine at 433 K utilizing principle component analyses of terahertz spectra collected at various points throughout the transition.[77,114] The increased accessibility to LFR spectrometers has enabled both low-frequency techniques to be used in a similar manner to characterize the temperature-dependent transitions of the five polymorphs of sulfathiazole.[117]

More recently, LFR spectroscopy has been effectively utilized to detect and track the temperature-dependent single-crystal to single-crystal reversible transitions between the conformational polymorphs of desloratadine.[109] Additionally, LFR spectroscopy paired with solid-state DFT methods has been used to identify the transformation pathway and energetics behind the observed temperature-induced phase transition of 1,2,4,5-tetrabromobenzene, an organic crystal that undergoes a rapid structural transition when heated and suddenly releases built-up mechanical strain, causing the crystals to physically jump.[23] In this work, a low-frequency vibration at 15 cm^{-1} was found to map out the transformation pathway, enabling understanding the mechanism and energetics of the phase transition, with the authors referring to this particular mode as a "gateway vibration".

Suzuki et al. utilized time-dependent terahertz spectroscopy to establish the temperature-induced transition kinetics between polymorphic phases of crystalline cyclohexanol from 150 to 330 K.[158] Two-dimensional plots of first derivatives of terahertz absorbance with respect to time revealed the stepwise kinetic behavior behind the transitions. This is shown for the two-step transition between Phases I and III via an intermediate in Figure 5.

https://doi.org/10.1021/acs.cgd.1c00850
Cryst. Growth Des. 2022, 22, 939−953

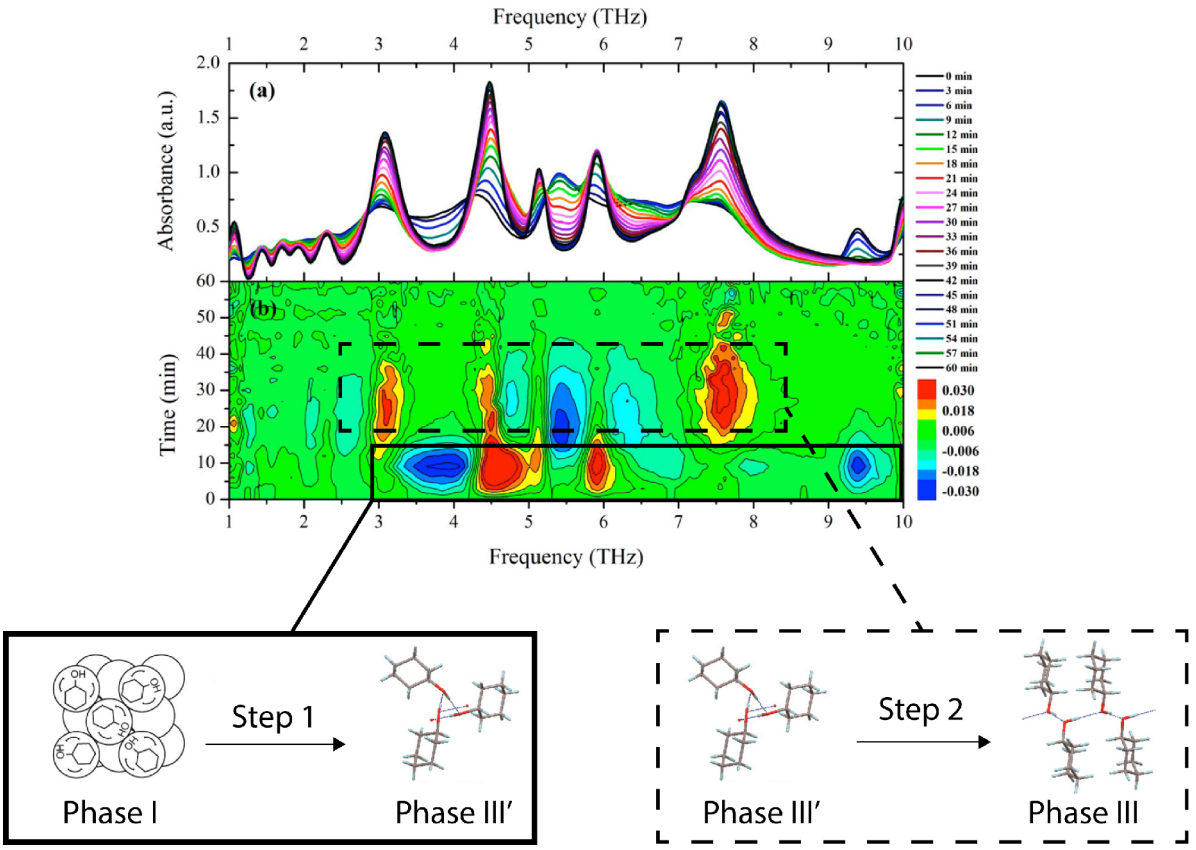

Figure 5. (a) Terahertz spectra of temperature-induced two-step transformation of cyclohexanol from Phase I (274 K) to III (233 K) via an intermediate over 60 min. (b) The first derivative of the terahertz spectra for this transformation with respect to time, where red and blue areas correspond to an increase and decrease in spectral intensity, respectively. Figure adapted with permission from ref 158. Copyright 2014 American Chemical Society.

Understanding transformation pathways is especially complicated in disordered systems where structural details are limited or unclear. The sensitivity of low-frequency spectroscopy provides a unique approach to understanding disorder in crystalline materials. In many cases, growing large single crystals of a material is not possible, or materials might be disordered to the extent that a single-crystal XRD data set is not able to determine the specific three-dimensional structure of the material. Both low-frequency techniques can be used to probe the vibrational dynamics and, when coupled with theoretical models, can pinpoint the correct structure. This has been demonstrated for a variety of disordered molecular crystals including the ordered and disordered phases of camphor[159] and the conformational disorder in irbesartan.[160] A similar approach was used to deduce the high-temperature crystal structure and presumed phase transformation kinetics for barbituric acid dihydrate. From theoretical models and terahertz spectroscopy, Paul et al. determined that rather than undergoing a temperature-dependent phase change at high temperatures barbituric acid dihydrate exists in a thermally disordered state.[21] Low-frequency vibrational spectroscopy can even be used to confirm the structures of unknown materials, often in conjunction with other methods such as crystal structure prediction.[161]

Transformations between amorphous and crystalline phases are affected by several external factors including humidity, temperature, and pressure. In the presence or absence of humidity, solid-state hydration and dehydration processes will affect the long-range interactions of a solid material.[155] This change has been monitored with terahertz spectroscopy to determine the dehydration kinetics of glucose monohydrate and in studying the hydration and subsequent crystallization of amorphous anhydrous lactose.[162,163] Low-frequency spectroscopy has been especially popular in studying the solid-state isothermal transformations between crystalline and amorphous forms of pharmaceuticals such as acetaminophen, caffeine, and indomethacin, to name a few.[118,164−166] The transformations of indomethacin, a nonsteroidal anti-inflammatory drug, between the crystalline and amorphous phase, has been the focus of numerous low-frequency spectroscopic studies to evaluate the transition mechanisms and kinetics underpinning this process. LFR spectroscopy has been demonstrated to be particularly sensitive in detection of the first traces and quantification of crystallization to the stable γ-phase at a temperature below the glass transition temperature.[27,142]

In addition to these phase transitions, terahertz techniques have been used to monitor solid-state reactions[167] and track cocrystal formation.[168−170] An early demonstration of this capability was the quantitative monitoring of the mechanochemical formation of a cocrystal between phenazine and mesaconic acid. Lien Nguyen et al. utilized an identifying spectral feature at 1.2 THz to deduce that mechanochemical cocrystal formation began with an amorphization of the individual components through grinding, with the amorphous component crystallizing as the cocrystal after a few days.[171]

Finally, the direct link between particular terahertz vibrations and the phase transformations has opened the door to utilizing terahertz radiation alone to drive these

https://doi.org/10.1021/acs.cgd.1c00850
Cryst. Growth Des. 2022, 22, 939−953

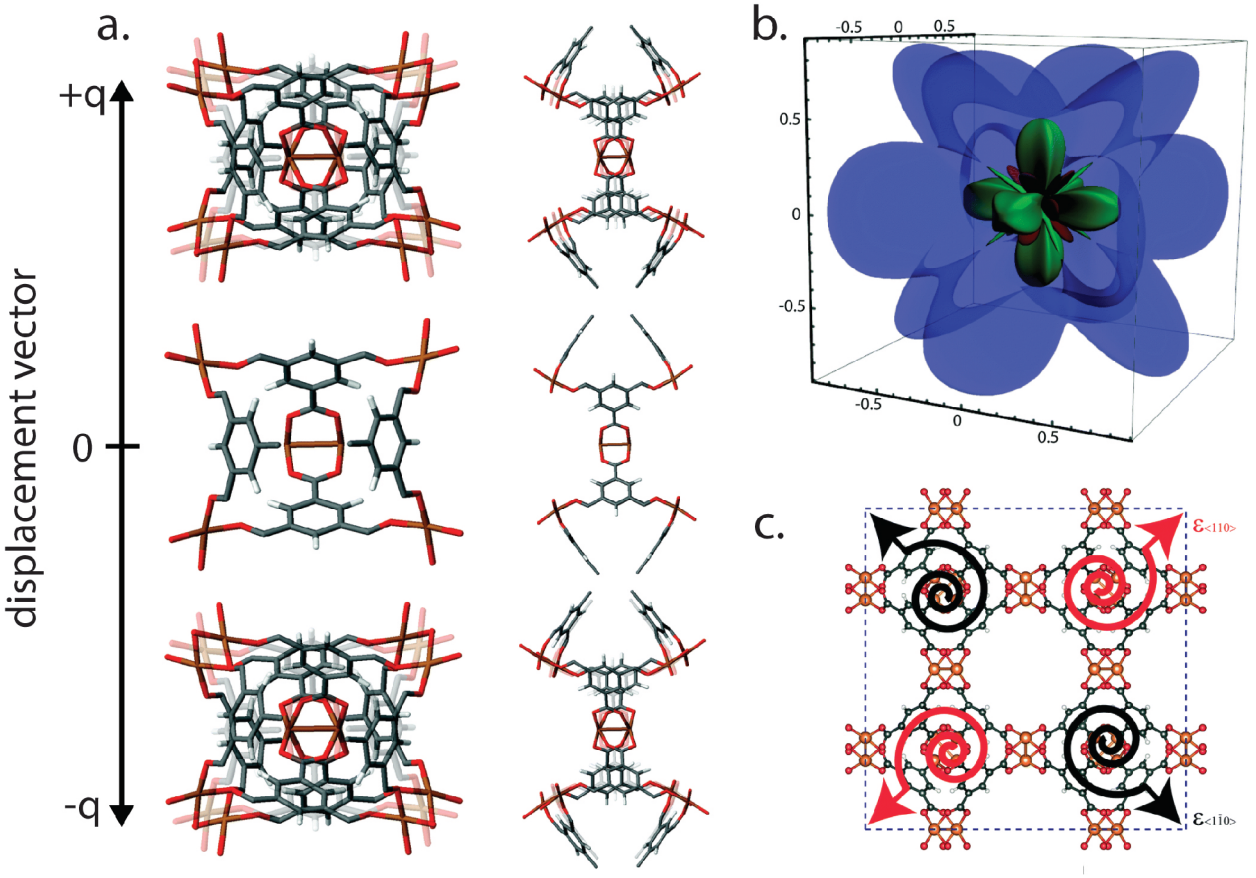

Figure 6. (a) Rotational motion along the displacement coordinate for the low-energy collective vibration at 16.32 cm^{-1} in HKUST-1 visualized along the <100> and <110> directions. (b) Predicted Poisson's ratio depiction in HKUST-1, where green and red regions correspond to positive and negative ratios, respectively. Blue regions denote maximum Poisson's ratio. (c) Proposed mechanism of the auxetic response associated with the low-energy collective vibration at 16.32 cm^{-1}. Figure adapted with permission from ref 35. Copyright 2016 Royal Society of Chemistry.

processes in a variety of complex materials.[28,172] In one example, high-field terahertz pulses from a free-electron laser were shown to promote crystallization of indomethacin, an active pharmaceutical ingredient, from the amorphous state—even when cooled well-below the glass transition temperature.[173] In that work, not only did terahertz radiation drive crystallization but also the terahertz-induced crystallization process produced a different polymorphic form than what is generated via thermally induced transformations, suggesting terahertz radiation can preferentially guide crystal growth. A similar investigation by Hoshina et al. nondestructively induced rearrangements of intermolecular conformations and increased the crystallinity of polymers with terahertz irradiation generated by a free-electron laser.[26] Recently, Li et al. discovered that upon excitation of strontium titanate ($SrTiO_3$) with high-field ultrafast terahertz pulses, a previously unknown metastable ferroelectric phase is induced with a reduced symmetry compared to the stable form.[28] The metastable crystal, because of its structural changes, exhibits a unique terahertz spectrum than can be observed using standard terahertz transmissions measurements and ultimately highlights the utility of terahertz radiation for not only understanding lattice dynamics but also controlling them, opening the door to an entirely new area of research within the terahertz sciences.

Probing the Mechanical Response of Solids. In addition to mapping out phase transformation pathways, there are a number of examples in the literature where terahertz vibrational motions have been directly linked to bulk material properties and functions.[15,35,174,175] This is a result of years of efforts devoted to the acquisition of experimental low-frequency vibrational spectra, coupled with advances in simulation methods for interpreting the experimental data, and represents the current state-of-the-art in the field of terahertz vibrational spectroscopy.

One eloquent application of low-frequency vibrational spectroscopy involves the mechanical properties of solids.[176] In general, the mechanical response of materials can be quantified through an understanding of the elastic tensor, which originates from Hooke's law.[177] The elastic tensor contains terms (elastic constants) that relate the change in energy of a system with respect to an applied strain (or deformation),

$$C_{vu} = \frac{1}{V}\frac{\partial^2 E}{\partial \eta_v \partial \eta_u}\bigg|_0 \tag{3}$$

where C_{vu} are the elastic constants, E is the total energy, η are the strain tensors, and the subscripts v and u represent the direction of the applied strain.[178,179] Thus, the elastic tensor elements provide insight into how a material responds to an applied strain. From eq 3, it can be observed that the calculation of elastic constants is very similar to the determination of vibrational force constants, which also arises from Hooke's law, with the vibrational expression given by,

https://doi.org/10.1021/acs.cgd.1c00850
Cryst. Growth Des. 2022, 22, 939−953

$$k_{vu} = \left.\frac{\partial^2 E}{\partial R_v \partial R_u}\right|_0 \quad (4)$$

where k is the vibrational force constant and R is the displacement vector for a particular coordinate. While eqs 3 and 4 are not identical, they are very similar—with the key difference being the nature of the applied displacement—with C arising from the deformation of the unit cell, while k relies on deformation of only pairs of atoms.[180] Thus, all vibrational modes can be related to elastic properties. However, this does not provide much utility for a majority of vibrational modes, since most vibrations are quite localized in nature, effectively providing insight into the elastic nature of chemical bonds, for example. However, low-frequency vibrational dynamics are large-amplitude and intermolecular, which implies that in some cases terahertz vibrations can be effective probes of bulk elasticity since they inherently probe intermolecular strain.

The link between lattice dynamics and elasticity has been increasingly reported in the literature over the latter half of the past decade.[33,181−184] In a report by Ryder et al., the connections between terahertz motions and anomalous mechanical properties in metal−organic frameworks (MOFs) were elucidated.[185] In that work, qualitative comparisons between particular vibrational modes and elastic constants were discussed, although no formal link between the two was established. Following this report, Ryder et al. examined the deformation mechanisms in the paddle-wheel MOF, HKUST-1, believed to dictate mechanical properties, including Young's and shear moduli and Poisson's ratio. The results reinforced the link between low-frequency motions such as soft modes and intrinsic shear distortions and elastic phenomena. An example of this connection is highlighted in Figure 6 where the low-frequency rotational motion that gives rise to a feature at 16.32 cm^{-1} was linked to the transverse and axial strains under deformation, which is described by Poisson's ratio. Interestingly, as seen in Figure 6, the Poisson's ratio for HKUST-1 in some crystalline directions is predicted to be negative indicating auxetic behavior. In a related work involving poly-L-proline helices, a framework for directly obtaining the bulk Young's modulus of solids from vibrational force constants was reported.[34] In that study, the presence of large-amplitude "spring-type" vibrations of the polymer helices provided a quantitative description of the mechanical properties of the material, which were in excellent agreement with the calculated values from dedicated elastic calculations.

From these two studies, this area of the terahertz sciences has begun to grow,[90,186] as contactless and nondestructive spectroscopic experiments are more easily performed than direct mechanical measurements, which often require the growth of large single crystals coupled with the precise manipulation of crystalline orientation over the course of the experiment. An investigation into the nonlinear mechanical response as a function of pressure in ZIF-8, a common MOF, by Zhang et al. found that a single terahertz vibrational mode served as indicator of the compressibility of the material under pressure.[22] Maul et al. developed a new theoretical algorithm for decomposing the elastic tensor elements into contributions from individual normal modes, providing for the first time a means of unifying low-frequency vibrational spectroscopy and the mechanical response of solids.[187] That work relied on both experimental IR and Raman spectroscopy data, as some crucial vibrational modes were either Raman- or IR-active, highlighting the complementary nature of the two techniques.

Finally, as the clear link between terahertz dynamics and the description of mechanical response in solids was established, this has enabled more complex investigations to be considered. One example is the ability to determine the thermomechanical response of materials or how the mechanical properties of materials change as a function of temperature.[188,189] While traditional experimental probes of elasticity are not readily used with varying temperatures, the ability to acquire variable temperature spectroscopic data is relatively straightforward. Thus, by capturing how low-frequency dynamics change upon heating or cooling, a measure of how the mechanical response changes can be obtained by extension.[190] This was highlighted in a recent work by Banks et al., where the thermomechanical response of a pair of organic semiconducting crystals was reported.[36] The investigation, which relied on experimental terahertz vibrational spectroscopy and quasi-harmonic DFT simulations, provided an excellent agreement with the room-temperature mechanical properties of crystalline rubrene, which were previously determined with Brillouin light scattering experiments.[191] The success of the method was then extended to a second material, ([1]benzothieno[3,2-*b*][1]benzothiophene) (BTBT), with an overview of the data used to generate the thermomechanical response, as well as the three-dimensional Young's moduli as a function of temperature, shown in Figure 7. Overall, this work helps to showcase how the utilization of terahertz vibrational dynamics can provide insight into complex phenomena that rely on fundamental intermolecular forces and how the field is regularly expanding beyond its core use into new and diverse applications.

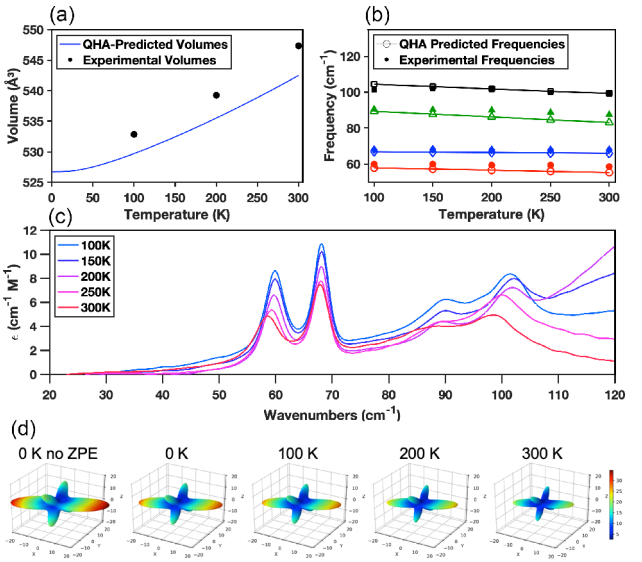

Figure 7. Thermoelastic response of BTBT determined using QHA simulations and terahertz spectroscopy. (a) QHA-predicted (blue) and experimental unit cell volumes. (b) Experimental (markers) and predicted (lines) temperature-dependent terahertz spectroscopy peak positions, with the spectra shown in (c). (d) Three-dimensional Young's moduli as a function of temperature. Figure adapted with permission from ref 36. Copyright 2020 Royal Society of Chemistry.

https://doi.org/10.1021/acs.cgd.1c00850
Cryst. Growth Des. 2022, 22, 939−953

CONCLUSION

Originating as boutique techniques, the terahertz sciences have evolved over the past few decades, driven largely by technological advances in ultrafast lasers and high-performance computing. The pioneers in the early 21st century methodically laid the groundwork for the current state of affairs by creating, modifying, and improving experimental and theoretical methodologies, while helping to establish standard practices, all of which have contributed to making the terahertz sciences more accessible than ever before. Over the past few years, the community has began to evolve and expand beyond traditional disciplines and applications, largely due to the increased understanding of the nature of terahertz vibrational motions. This Perspective does not exhaustively describe the many different applications of low-frequency dynamics to bulk material phenomena, and there are new and innovative examples in the literature on a regular basis. With any growing method, there are areas where improvement in the terahertz sciences would only help to further the field. For example, the limit of many commercial terahertz time-domain spectrometers to rather narrow bandwidths (0.3−6.0 THz) must be improved upon in order to be more generally applicable to a wide variety of materials. In terms of LFR, oftentimes acquiring Raman shifts in the THz region requires the use of a single laser source, which can be problematic for fluorescent materials, for example. Finally, the ability to generate ultrahigh terahertz electric fields in traditional academic laboratories represents the next frontier, as currently there is a large gap between the pulse energies achievable with academic lasers and those obtainable at large international facilities such as free-electron lasers. However, in spite of these challenges, the terahertz community is extremely healthy and active, and there is no doubt that as the techniques become more mainstream new and exciting applications will be developed, continuing the growth and innovation that have been ongoing since the late 1980s.

AUTHOR INFORMATION

Corresponding Author

Michael T. Ruggiero − *Department of Chemistry, University of Vermont, Burlington, Vermont 05405, United States;* orcid.org/0000-0003-1848-2565; Phone: +1 (802) 656-0276; Email: Michael.Ruggiero@uvm.edu

Author

Elyse M. Kleist − *Department of Chemistry, University of Vermont, Burlington, Vermont 05405, United States;* orcid.org/0000-0001-8596-659X

Complete contact information is available at: https://pubs.acs.org/10.1021/acs.cgd.1c00850

Notes

The authors declare no competing financial interest.

ACKNOWLEDGMENTS

The authors thank the National Science Foundation (CHE-2055402 and DMR-2046483) and the University of Vermont for support.

REFERENCES

(1) Baxter, J. B.; Guglietta, G. W. Terahertz spectroscopy. *Anal. Chem.* **2011**, *83*, 4342−4368.

(2) Dhillon, S. S.; et al. The 2017 terahertz science and technology roadmap. *J. Phys. D: Appl. Phys.* **2017**, *50*, 043001.

(3) Gente, R.; Koch, M. Monitoring leaf water content with THz and sub-THz waves. *Plant Methods* **2015**, *11*, 15.

(4) Matsunaga, R.; Hamada, Y. I.; Makise, K.; Uzawa, Y.; Terai, H.; Wang, Z.; Shimano, R. Higgs amplitude mode in the BCS superconductors Nb_1-xTixN induced by terahertz pulse excitation. *Phys. Rev. Lett.* **2013**, *111*, 057002.

(5) Zhang, W.; Maldonado, P.; Jin, Z.; Seifert, T. S.; Arabski, J.; Schmerber, G.; Beaurepaire, E.; Bonn, M.; Kampfrath, T.; Oppeneer, P. M.; Turchinovich, D. Ultrafast terahertz magnetometry. *Nat. Commun.* **2020**, *11*, 11.

(6) Lin, H.; Russell, B. P.; Bawuah, P.; Zeitler, J. A. Sensing water absorption in hygrothermally aged epoxies with terahertz time-domain spectroscopy. *Anal. Chem.* **2021**, *93*, 2449−2455.

(7) Nahar, S.; Mohamed, A.; Ropagnol, X.; Hassanpour, A.; Kiwa, T.; Ozaki, T.; Gauthier, M. A. Non-invasive, label-free, and quantitative monitoring of lipase kinetics using Terahertz emission technology. *Biotechnol. Bioeng.* **2021**, DOI: 10.1002/bit.27893.

(8) Shen, Y.-C. Terahertz pulsed spectroscopy and imaging for pharmaceutical applications: A review. *Int. J. Pharm.* **2011**, *417*, 48−60.

(9) Elayan, H.; Stefanini, C.; Shubair, R. M.; Jornet, J. M. End-to-end noise model for intra-body terahertz nanoscale communication. *IEEE Trans. NanoBioscience* **2018**, *17*, 464−473.

(10) Koch Dandolo, C. L.; Picollo, M.; Cucci, C.; Ginanni, M.; Prandi, E.; Scudieri, M.; Jepsen, P. U. Insights on the side panels of the Franciscan triptych by Fra Angelico using terahertz time-domain imaging (THz-TDI). *J. Infrared, Millimeter, Terahertz Waves* **2017**, *38*, 413−424.

(11) Dandolo, C. L. K.; Guillet, J.-P.; Ma, X.; Fauquet, F.; Roux, M.; Mounaix, P. Terahertz frequency modulated continuous wave imaging advanced data processing for art painting analysis. *Opt. Express* **2018**, *26*, 5358.

(12) Bardon, T.; May, R. K.; Jackson, J. B.; Beentjes, G.; de Bruin, G.; Taday, P. F.; Strlič, M. Contrast in terahertz images of archival documents—part I: Influence of the optical parameters from the ink and support. *J. Infrared, Millimeter, Terahertz Waves* **2017**, *38*, 443−466.

(13) Bardon, T.; May, R. K.; Taday, P. F.; Strlič, M. Contrast in terahertz images of archival documents—part II: Influence of topographic features. *J. Infrared, Millimeter, Terahertz Waves* **2017**, *38*, 467−482.

(14) Kleine-Ostmann, T.; Nagatsuma, T. A review on terahertz communications research. *J. Infrared, Millimeter, Terahertz Waves* **2011**, *32*, 143−171.

(15) Cheatum, C. M. Low-Frequency protein motions coupled to catalytic sites. *Annu. Rev. Phys. Chem.* **2020**, *71*, 267−288.

(16) Day, G. M.; Zeitler, J. A.; Jones, W.; Rades, T.; Taday, P. F. Understanding the influence of polymorphism on phonon spectra: Lattice dynamics calculations and terahertz spectroscopy of carbamazepine. *J. Phys. Chem. B* **2006**, *110*, 447−456.

(17) Chieng, N.; Rades, T.; Aaltonen, J. An overview of recent studies on the analysis of pharmaceutical polymorphs. *J. Pharm. Biomed. Anal.* **2011**, *55*, 618−644.

(18) Roy, S.; Chamberlin, B.; Matzger, A. J. Polymorph discrimination using low wavenumber Raman spectroscopy. *Org. Process Res. Dev.* **2013**, *17*, 976−980.

(19) Berzins, K.; Sutton, J. J.; Fraser-Miller, S. J.; Rades, T.; Korter, T. M.; Gordon, K. C. Solving the computational puzzle: Toward a pragmatic pathway for modeling low-energy vibrational modes of pharmaceutical crystals. *Cryst. Growth Des.* **2020**, *20*, 6947−6955.

(20) Ruggiero, M. T.; Zhang, W.; Bond, A. D.; Mittleman, D. M.; Zeitler, J. A. Uncovering the connection between low-frequency dynamics and phase transformation phenomena in molecular solids. *Phys. Rev. Lett.* **2018**, *120*, 196002.

(21) Paul, M. E.; da Silva, T. H.; King, M. D. True polymorphic phase transition or dynamic crystal disorder? An investigation into the

unusual phase behavior of barbituric acid dihydrate. *Cryst. Growth Des.* **2019**, *19*, 4745−4753.
(22) Zhang, W.; Maul, J.; Vulpe, D.; Moghadam, P. Z.; Fairen-Jimenez, D.; Mittleman, D. M.; Zeitler, J. A.; Erba, A.; Ruggiero, M. T. Probing the mechanochemistry of metal−organic frameworks with low-frequency vibrational spectroscopy. *J. Phys. Chem. C* **2018**, *122*, 27442−27450.
(23) Zaczek, A. J.; Catalano, L.; Naumov, P.; Korter, T. M. Mapping the polymorphic transformation gateway vibration in crystalline 1,2,4,5-tetrabromobenzene. *Chem. Sci.* **2019**, *10*, 1332−1341.
(24) Zhang, W.; Song, Z.; Ruggiero, M. T.; Mittleman, D. M. Terahertz vibrational motions mediate gas uptake in organic clathrates. *Cryst. Growth Des.* **2020**, *20*, 5638−5643.
(25) Tanno, T.; Watanabe, Y.; Umeno, K.; Matsuoka, A.; Matsumura, H.; Odaka, M.; Ogawa, N. In situ observation of gas adsorption onto ZIF-8 using terahertz waves. *J. Phys. Chem. C* **2017**, *121*, 17921−17924.
(26) Hoshina, H.; Suzuki, H.; Otani, C.; Nagai, M.; Kawase, K.; Irizawa, A.; Isoyama, G. Polymer morphological change induced by terahertz irradiation. *Sci. Rep.* **2016**, *6*, 27180.
(27) Walker, G.; Römann, P.; Poller, B.; Löbmann, K.; Grohganz, H.; Rooney, J. S.; Huff, G. S.; Smith, G. P. S.; Rades, T.; Gordon, K. C.; Strachan, C. J.; Fraser-Miller, S. J. Probing pharmaceutical mixtures during milling: The potency of low-frequency Raman spectroscopy in identifying disorder. *Mol. Pharmaceutics* **2017**, *14*, 4675−4684.
(28) Li, X.; Qiu, T.; Zhang, J.; Baldini, E.; Lu, J.; Rappe, A. M.; Nelson, K. A. Terahertz field−induced ferroelectricity in quantum paraelectric $SrTiO_3$. *Science* **2019**, *364*, 1079−1082.
(29) Turton, D. A.; Senn, H. M.; Harwood, T.; Lapthorn, A. J.; Ellis, E. M.; Wynne, K. Terahertz underdamped vibrational motion governs protein-ligand binding in solution. *Nat. Commun.* **2014**, *5*, 3999.
(30) Salén, P.; Basini, M.; Bonetti, S.; Hebling, J.; Krasilnikov, M.; Nikitin, A. Y.; Shamuilov, G.; Tibai, Z.; Zhaunerchyk, V.; Goryashko, V. Matter manipulation with extreme terahertz light: Progress in the enabling THz technology. *Phys. Rep.* **2019**, *836*−*837*, 1−74.
(31) Sosorev, A. Y.; Parashchuk, O. D.; Tukachev, N. V.; Maslennikov, D. R.; Dominskiy, D. I.; Borshchev, O. V.; Polinskaya, M. S.; Skorotetcky, M. S.; Kharlanov, O. G.; Paraschuk, D. Y. Suppression of dynamic disorder by electrostatic interactions in structurally close organic semiconductors. *Phys. Chem. Chem. Phys.* **2021**, *23*, 15485−15491.
(32) Schweicher, G.; et al. Chasing the "killer" phonon mode for the rational design of low-disorder, high-mobility molecular semiconductors. *Adv. Mater.* **2019**, *31*, 1902407.
(33) Maul, J.; Ongari, D.; Moosavi, S. M.; Smit, B.; Erba, A. Thermoelasticity of flexible organic crystals from quasi-harmonic lattice dynamics: The case of copper(II) acetylacetonate. *J. Phys. Chem. Lett.* **2020**, *11*, 8543−8548.
(34) Ruggiero, M. T.; Sibik, J.; Orlando, R.; Zeitler, J. A.; Korter, T. M. Measuring the elasticity of poly-l-proline helices with terahertz spectroscopy. *Angew. Chem.* **2016**, *128*, 6991−6995.
(35) Ryder, M. R.; Civalleri, B.; Cinque, G.; Tan, J.-C. Discovering connections between terahertz vibrations and elasticity underpinning the collective dynamics of the HKUST-1 metal−organic framework. *CrystEngComm* **2016**, *18*, 4303−4312.
(36) Banks, P. A.; Maul, J.; Mancini, M. T.; Whalley, A. C.; Erba, A.; Ruggiero, M. T. Thermoelasticity in organic semiconductors determined with terahertz spectroscopy and quantum quasi-harmonic simulations. *J. Mater. Chem. C* **2020**, *8*, 10917−10925.
(37) Low, F. J. Low-temperature germanium bolometer. *J. Opt. Soc. Am.* **1961**, *51*, 1300−1304.
(38) Chanin, G.; Torre, J. P.; Peccoud, L. Low heat capacity He^3-cooled bolometers of differentiated structure. *Infrared Phys.* **1978**, *18*, 657−662.
(39) Haller, E. E. Advanced far-infrared detectors. *Infrared Phys. Technol.* **1994**, *35*, 127−146.
(40) Auston, D. H. Picosecond optoelectronic switching and gating in silicon. *Appl. Phys. Lett.* **1975**, *26*, 101−103.
(41) Auston, D. H.; Johnson, A. M.; Smith, P. R.; Bean, J. C. Picosecond optoelectronic detection, sampling, and correlation measurements in amorphous semiconductors. *Appl. Phys. Lett.* **1980**, *37*, 371−373.
(42) Auston, D. H.; Smith, P. R. Generation and detection of millimeter waves by picosecond photoconductivity. *Appl. Phys. Lett.* **1983**, *43*, 631−633.
(43) Auston, D. H.; Cheung, K. P.; Smith, P. R. Picosecond photoconducting Hertzian dipoles. *Appl. Phys. Lett.* **1984**, *45*, 284−286.
(44) Fattinger, C.; Grischkowsky, D. Terahertz beams. *Appl. Phys. Lett.* **1989**, *54*, 490−492.
(45) de L. Kronig, R. On the theory of dispersion of x-rays. *J. Opt. Soc. Am.* **1926**, *12*, 547−557.
(46) Beck, M.; Walmsley, I. A.; Kafka, J. D. Group delay measurements of optical components near 800 nm. *IEEE J. Quantum Electron.* **1991**, *27*, 2074−2081.
(47) Lucarini, V.; Saarinen, J.; Peiponen, K.; Vartiainen, E. *Kramers-Kronig Relations in Optical Materials Research*; Springer Berlin Heidelberg, 2005.
(48) El Haddad, J.; Bousquet, B.; Canioni, L.; Mounaix, P. Review in terahertz spectral analysis. *TrAC, Trends Anal. Chem.* **2013**, *44*, 98−105.
(49) Fukuchi, T.; Fuse, N.; Fujii, T.; Okada, M.; Fukunaga, K.; Mizuno, M. Measurement of topcoat thickness of thermal barrier coating for gas turbines using terahertz waves. *Electr. Eng. JPN* **2013**, *183*, 1−9.
(50) Lee, Y. *Principles of Terahertz Science and Technology*; Springer US, 2009.
(51) Wu, Q.; Zhang, X. Free-space electro-optic sampling of terahertz beams. *Appl. Phys. Lett.* **1995**, *67*, 3523−3525.
(52) Gallot, G.; Grischkowsky, D. Electro-optic detection of terahertz radiation. *J. Opt. Soc. Am. B* **1999**, *16*, 1204−1212.
(53) Gallot, G.; Zhang, J.; McGowan, R. W.; Jeon, T.-I.; Grischkowsky, D. Measurements of the THz absorption and dispersion of ZnTe and their relevance to the electro-optic detection of THz radiation. *Appl. Phys. Lett.* **1999**, *74*, 3450−3452.
(54) Auston, D. H.; Nuss, M. C. Electrooptical generation and detection of femtosecond electrical transients. *IEEE J. Quantum Electron.* **1988**, *24*, 184−197.
(55) Nahata, A.; Auston, D. H.; Heinz, T. F.; Wu, C. Coherent detection of freely propagating terahertz radiation by electro-optic sampling. *Appl. Phys. Lett.* **1996**, *68*, 150−152.
(56) Darrow, J. T.; Zhang, X.; Auston, D. H.; Morse, J. D. Saturation properties of large-aperture photoconducting antennas. *IEEE J. Quantum Electron.* **1992**, *28*, 1607−1616.
(57) You, D.; Jones, R. R.; Bucksbaum, P. H.; Dykaar, D. R. Generation of high-power sub-single-cycle 500-fs electromagnetic pulses. *Opt. Lett.* **1993**, *18*, 290−292.
(58) Jepsen, P. U.; Jacobsen, R. H.; Keiding, S. R. Generation and detection of terahertz pulses from biased semiconductor antennas. *J. Opt. Soc. Am. B* **1996**, *13*, 2424−2436.
(59) Lewis, R. A. A review of terahertz detectors. *J. Phys. D: Appl. Phys.* **2019**, *52*, 433001.
(60) Hafez, H. A.; Chai, X.; Ibrahim, A.; Mondal, S.; Férachou, D.; Ropagnol, X.; Ozaki, T. Intense terahertz radiation and their applications. *J. Opt.* **2016**, *18*, 093004.
(61) Parrott, E. P. J.; Zeitler, J. A. Terahertz time-domain and low-frequency Raman spectroscopy of organic materials. *Appl. Spectrosc.* **2015**, *69*, 1−25.
(62) Raman, C. V.; Krishnan, K. S. A new type of secondary radiation. *Nature* **1928**, *121*, 501−502.
(63) Venkateswaran, C. S. Low frequency Raman lines in organic crystals. *Proc. - Indian Acad. Sci., Sect. A* **1938**, *8*, 448−459.
(64) Harris, D.; Bertolucci, M. *Symmetry and Spectroscopy: An Introduction to Vibrational and Electronic Spectroscopy*; Dover Books on Chemistry Series; Dover Publications, 1989.

https://doi.org/10.1021/acs.cgd.1c00850
Cryst. Growth Des. 2022, 22, 939−953

(65) Wilson, E. B.; Decius, J. C.; Cross, P. C.; Sundheim, B. R. Molecular vibrations: The theory of infrared and Raman vibrational spectra. *J. Electrochem. Soc.* **1955**, *102*, 235C.
(66) Carriere, J. New opportunities in low-frequency Raman spectroscopy. *Photon. Spectra* **2011**, *45*, 48−53.
(67) Berzins, K.; Fraser-Miller, S. J.; Gordon, K. C. Recent advances in low-frequency Raman spectroscopy for pharmaceutical applications. *Int. J. Pharm.* **2021**, *592*, 120034.
(68) Moser, C.; Havermeyer, F. Ultra-narrow-band tunable laserline notch filter. *Appl. Phys. B: Lasers Opt.* **2009**, *95*, 597−601.
(69) Moser, C.; Havermeyer, F. Compact Raman spectrometer system for low-frequency spectroscopy. In *Optical Components and Materials VII*; SPIE, 2010; p 75980S.
(70) Hédoux, A. Recent developments in the Raman and infrared investigations of amorphous pharmaceuticals and protein formulations: A review. *Adv. Drug Delivery Rev.* **2016**, *100*, 133−146.
(71) Socrates, G. *Infrared and Raman Characteristic Group Frequencies: Tables and Charts*; John Wiley & Sons, 2004.
(72) Baenziger, N. C.; Duax, W. L. Crystal structure and molecular motion of solid carbon disulfide. *J. Chem. Phys.* **1968**, *48*, 2974−2981.
(73) Zhang, F.; Wang, H.-W.; Tominaga, K.; Hayashi, M. Intramolecular vibrations in low-frequency normal modes of amino acids: l-alanine in the neat solid state. *J. Phys. Chem. A* **2015**, *119*, 3008−3022.
(74) Ruggiero, M. T. Invited review: Modern methods for accurately simulating the terahertz spectra of solids. *J. Infrared, Millimeter, Terahertz Waves* **2020**, *41*, 491−528.
(75) Hasnip, P. J.; Refson, K.; Probert, M. I. J.; Yates, J. R.; Clark, S. J.; Pickard, C. J. Density functional theory in the solid state. *Philos. Trans. R. Soc., A* **2014**, *372*, 20130270.
(76) Allis, D. G.; Prokhorova, D. A.; Korter, T. M. Solid-state modeling of the terahertz spectrum of the high explosive HMX. *J. Phys. Chem. A* **2006**, *110*, 1951−9.
(77) Zeitler, J. A.; Newnham, D. A.; Taday, P. F.; Strachan, C. J.; Pepper, M.; Gordon, K. C.; Rades, T. Temperature dependent terahertz pulsed spectroscopy of carbamazepine. *Thermochim. Acta* **2005**, *436*, 71−77.
(78) Zhang, Y.; Peng, X. H.; Chen, Y.; Chen, J.; Curioni, A.; Andreoni, W.; Nayak, S. K.; Zhang, X. C. A first principle study of terahertz (THz) spectra of acephate. *Chem. Phys. Lett.* **2008**, *452*, 59−66.
(79) Pascale, F.; Zicovich-Wilson, C. M.; López Gejo, F.; Civalleri, B.; Orlando, R.; Dovesi, R. The calculation of the vibrational frequencies of crystalline compounds and its implementation in the CRYSTAL code. *J. Comput. Chem.* **2004**, *25*, 888−897.
(80) Zicovich-Wilson, C.; Pascale, F.; Roetti, C.; Saunders, V.; Orlando, R.; Dovesi, R. Calculation of the vibration frequencies of α-quartz: The effect of Hamiltonian and basis set. *J. Comput. Chem.* **2004**, *25*, 1873−1881.
(81) Becke, A. D.; Johnson, E. R. A density functional model of the dispersion interaction. *J. Chem. Phys.* **2005**, *123*, 154101.
(82) Grimme, S. Accurate description of van der Waals complexes by density functional theory including empirical corrections. *J. Comput. Chem.* **2004**, *25*, 1463−1473.
(83) Grimme, S.; Antony, J.; Ehrlich, S.; Krieg, H. A consistent and accurate *ab initio* parametrization of density functional dispersion correction (DFT-D) for the 94 elements H-Pu. *J. Chem. Phys.* **2010**, *132*, 154104.
(84) Grimme, S. Density functional theory with London dispersion corrections. *Wiley Interdiscip. Rev.: Comput. Mol. Sci.* **2011**, *1*, 211−228.
(85) Kristyán, S.; Pulay, P. Can (semi)local density functional theory account for the London dispersion forces? *Chem. Phys. Lett.* **1994**, *229*, 175−180.
(86) Otero-de-la-Roza, A.; LeBlanc, L. M.; Johnson, E. R. What is "many-body" dispersion and should I worry about it? *Phys. Chem. Chem. Phys.* **2020**, *22*, 8266−8276.
(87) Grimme, S.; Ehrlich, S.; Goerigk, L. Effect of the damping function in dispersion corrected density functional theory. *J. Comput. Chem.* **2011**, *32*, 1456−1465.
(88) Elrod, M. J.; Saykally, R. J. Many-body effects in intermolecular forces. *Chem. Rev.* **1994**, *94*, 1975−1997.
(89) Hutereau, M.; Banks, P. A.; Slater, B.; Zeitler, J. A.; Bond, A. D.; Ruggiero, M. T. Resolving Anharmonic Lattice Dynamics in Molecular Crystals with X-Ray Diffraction and Terahertz Spectroscopy. *Phys. Rev. Lett.* **2020**, *125*, 103001.
(90) Ruggiero, M. T.; Zeitler, J. A.; Erba, A. Intermolecular anharmonicity in molecular crystals: interplay between experimental low-frequency dynamics and quantum quasi-harmonic simulations of solid purine. *Chem. Commun.* **2017**, *53*, 3781−3784.
(91) Erba, A.; Maul, J.; Ferrabone, M.; Carbonnière, P.; Rérat, M.; Dovesi, R. Anharmonic Vibrational States of Solids from DFT Calculations. Part I: Description of the Potential Energy Surface. *J. Chem. Theory Comput.* **2019**, *15*, 3755−3765.
(92) Erba, A.; Maul, J.; Ferrabone, M.; Dovesi, R.; Rérat, M.; Carbonnière, P. Anharmonic Vibrational States of Solids from DFT Calculations. Part II: Implementation of the VSCF and VCI Methods. *J. Chem. Theory Comput.* **2019**, *15*, 3766−3777.
(93) Dovesi, R.; Erba, A.; Orlando, R.; Zicovich-Wilson, C. M.; Civalleri, B.; Maschio, L.; Rérat, M.; Casassa, S.; Baima, J.; Salustro, S.; Kirtman, B. Quantum-mechanical condensed matter simulations with CRYSTAL. *Wiley Interdiscip. Rev.: Comput. Mol. Sci.* **2018**, *8*. DOI: 10.1002/wcms.1360
(94) Hafner, J. *Ab-initio* simulations of materials using VASP: Density-functional theory and beyond. *J. Comput. Chem.* **2008**, *29*, 2044−2078.
(95) Giannozzi, P.; et al. QUANTUM ESPRESSO: A modular and open-source software project for quantum simulations of materials. *J. Phys.: Condens. Matter* **2009**, *21*, 395502.
(96) Giannozzi, P.; et al. Advanced capabilities for materials modelling with Quantum ESPRESSO. *J. Phys.: Condens. Matter* **2017**, *29*, 465901.
(97) Delley, B. From molecules to solids with the DMol3 approach. *J. Chem. Phys.* **2000**, *113*, 7756−7764.
(98) Kühne, T. D.; et al. CP2K: An electronic structure and molecular dynamics software package - Quickstep: Efficient and accurate electronic structure calculations. *J. Chem. Phys.* **2020**, *152*, 194103.
(99) VandeVondele, J.; Krack, M.; Mohamed, F.; Parrinello, M.; Chassaing, T.; Hutter, J. Quickstep: Fast and accurate density functional calculations using a mixed Gaussian and plane waves approach. *Comput. Phys. Commun.* **2005**, *167*, 103−128.
(100) Ruggiero, M. T.; Erba, A.; Orlando, R.; Korter, T. M. Origins of contrasting copper coordination geometries in crystalline copper sulfate pentahydrate. *Phys. Chem. Chem. Phys.* **2015**, *17*, 31023−31029.
(101) Dronskowski, R.; Bloechl, P. E. Crystal orbital Hamilton populations (COHP): energy-resolved visualization of chemical bonding in solids based on density-functional calculations. *J. Phys. Chem.* **1993**, *97*, 8617−8624.
(102) Neu, J.; Stone, E. A.; Spies, J. A.; Storch, G.; Hatano, A. S.; Mercado, B. Q.; Miller, S. J.; Schmuttenmaer, C. A. Terahertz spectroscopy of tetrameric peptides. *J. Phys. Chem. Lett.* **2019**, *10*, 2624−2628.
(103) Neu, J.; Schmuttenmaer, C. A. Terahertz spectroscopy and density functional theory investigation of the dipeptide l-carnosine. *J. Infrared, Millimeter, Terahertz Waves* **2020**, *41*, 1366−1377.
(104) Łuczyńska, K.; Drużbicki, K.; Runka, T.; Pałka, N.; Węsicki, J. Vibrational response of felodipine in the THz domain: Optical and neutron spectroscopy versus plane-wave DFT modeling. *J. Infrared, Millimeter, Terahertz Waves* **2020**, *41*, 1301−1336.
(105) Yamamoto, S.; Morisawa, Y.; Sato, H.; Hoshina, H.; Ozaki, Y. Quantum mechanical interpretation of intermolecular vibrational modes of crystalline poly-(R)-3-hydroxybutyrate observed in low-frequency Raman and terahertz spectra. *J. Phys. Chem. B* **2013**, *117*, 2180−2187.

(106) Druzbicki, K.; Pajzderska, A.; Chudoba, D.; Jenczyk, J.; Jarek, M.; Mielcarek, J.; Wasicki, J. Elucidating the structure of ranitidine hydrochloride form II: Insights from solid-state spectroscopy and ab initio simulations. *Cryst. Growth Des.* **2018**, *18*, 4671−4681.
(107) Druzbicki, K.; Mielcarek, J.; Kiwilsza, A.; Toupet, L.; Collet, E.; Pajzderska, A.; Wasicki, J. Computationally assisted (solid-state density functional theory) structural (X-ray) and vibrational spectroscopy (FT-IR, FT-RS, TDs-THz) characterization of the cardiovascular drug lacidipine. *Cryst. Growth Des.* **2015**, *15*, 2817−2830.
(108) Hobday, C. L.; Woodall, C. H.; Lennox, M. J.; Frost, M.; Kamenev, K.; Düren, T.; Morrison, C. A.; Moggach, S. A. Understanding the adsorption process in ZIF-8 using high pressure crystallography and computational modelling. *Nat. Commun.* **2018**, *9*, 1429.
(109) Srirambhatla, V. K.; Guo, R.; Dawson, D. M.; Price, S. L.; Florence, A. J. Reversible, two-step single-crystal to single-crystal phase transitions between desloratadine forms I, II, and III. *Cryst. Growth Des.* **2020**, *20*, 1800−1810.
(110) Takahashi, M.; Okamura, N.; Ding, X.; Shirakawa, H.; Minamide, H. Intermolecular hydrogen bond stretching vibrations observed in terahertz spectra of crystalline vitamins. *CrystEngComm* **2018**, *20*, 1960−1969.
(111) Iwata, K.; Karashima, M.; Ikeda, Y.; Inoue, M.; Fukami, T. Discrimination and quantification of sulfathiazole polytypes using low-frequency Raman spectroscopy. *CrystEngComm* **2018**, *20*, 1928−1934.
(112) McGoverin, C. M.; Rades, T.; Gordon, K. C. Recent pharmaceutical applications of Raman and terahertz spectroscopies. *J. Pharm. Sci.* **2008**, *97*, 4598−4621.
(113) Morissette, S. L.; Soukasene, S.; Levinson, D.; Cima, M. J.; Almarsson, O. Elucidation of crystal form diversity of the HIV protease inhibitor ritonavir by high-throughput crystallization. *Proc. Natl. Acad. Sci. U. S. A.* **2003**, *100*, 2180−2184.
(114) Zeitler, J. A.; Taday, P. F.; Gordon, K. C.; Pepper, M.; Rades, T. Solid-state transition mechanism in carbamazepine polymorphs by time-resolved terahertz spectroscopy. *ChemPhysChem* **2007**, *8*, 1924−1927.
(115) Taday, P. F.; Bradley, I. V.; Arnone, D. D.; Pepper, M. Using terahertz pulse spectroscopy to study the crystalline structure of a drug: A case study of the polymorphs of ranitidine hydrochloride. *J. Pharm. Sci.* **2003**, *92*, 831−838.
(116) Strachan, C. J.; Taday, P. F.; Newnham, D. A.; Gordon, K. C.; Zeitler, J. A.; Pepper, M.; Rades, T. Using terahertz pulsed spectroscopy to quantify pharmaceutical polymorphism and crystallinity. *J. Pharm. Sci.* **2005**, *94*, 837−846.
(117) Zeitler, J.; Newnham, D. A.; Taday, P. F.; Threlfall, T. L.; Lancaster, R. W.; Berg, R. W.; Strachan, C. J.; Pepper, M.; Gordon, K. C.; Rades, T. Characterization of temperature-induced phase transitions in five polymorphic forms of sulfathiazole by terahertz pulsed spectroscopy and differential scanning calorimetry. *J. Pharm. Sci.* **2006**, *95*, 2486−2498.
(118) Hédoux, A.; Decroix, A.-A.; Guinet, Y.; Paccou, L.; Derollez, P.; Descamps, M. Low- and high-frequency Raman investigations on caffeine: Polymorphism, disorder and phase transformation. *J. Phys. Chem. B* **2011**, *115*, 5746−5753.
(119) Bawuah, P.; Zeitler, J. A. Advances in terahertz time-domain spectroscopy of pharmaceutical solids: A review. *TrAC, Trends Anal. Chem.* **2021**, *139*, 116272.
(120) Larkin, P. J.; Dabros, M.; Sarsfield, B.; Chan, E.; Carriere, J. T.; Smith, B. C. Polymorph characterization of active pharmaceutical ingredients (APIs) using low-frequency Raman spectroscopy. *Appl. Spectrosc.* **2014**, *68*, 758−776.
(121) Carriere, J.; Heyler, R.; Smith, B. Polymorph identification and analysis using ultralow-frequency Raman spectroscopy. *Spectroscopy* **2013**, *26*, S44−S50.
(122) Lamshöft, M.; Ivanova, B.; Spiteller, M. Chemical identification and determination of sulfonamides in n-component solid mixtures within THz-region—Solid-state Raman spectroscopic and mass spectrometric study. *Talanta* **2011**, *85*, 2562−2575.
(123) King, M. D.; Buchanan, W. D.; Korter, T. M. Identification and quantification of polymorphism in the pharmaceutical compound diclofenac acid by terahertz spectroscopy and solid-state density functional theory. *Anal. Chem.* **2011**, *83*, 3786−3792.
(124) Inoue, M.; Hisada, H.; Koide, T.; Fukami, T.; Roy, A.; Carriere, J.; Heyler, R. Transmission low-frequency Raman spectroscopy for quantification of crystalline polymorphs in pharmaceutical tablets. *Anal. Chem.* **2019**, *91*, 1997−2003.
(125) Mah, P. T.; Fraser, S. J.; Reish, M. E.; Rades, T.; Gordon, K. C.; Strachan, C. J. Use of low-frequency Raman spectroscopy and chemometrics for the quantification of crystallinity in amorphous griseofulvin tablets. *Vib. Spectrosc.* **2015**, *77*, 10−16.
(126) Kleist, E. M.; Korter, T. M. Quantitative analysis of minium and vermilion mixtures using low-frequency vibrational spectroscopy. *Anal. Chem.* **2020**, *92*, 1211−1218.
(127) Lipiäinen, T.; Fraser-Miller, S. J.; Gordon, K. C.; Strachan, C. J. Direct comparison of low- and mid-frequency Raman spectroscopy for quantitative solid-state pharmaceutical analysis. *J. Pharm. Biomed. Anal.* **2018**, *149*, 343−350.
(128) Ueno, Y.; Rungsawang, R.; Tomita, I.; Ajito, K. Quantitative measurements of amino acids by terahertz time-domain transmission spectroscopy. *Anal. Chem.* **2006**, *78*, 5424−5428.
(129) Inoue, M.; Osada, T.; Hisada, H.; Koide, T.; Fukami, T.; Roy, A.; Carriere, J.; Heyler, R. Solid-state quantification of cocrystals in pharmaceutical tablets using transmission low-frequency Raman spectroscopy. *Anal. Chem.* **2019**, *91*, 13427−13432.
(130) Hakey, P. M.; Allis, D. G.; Hudson, M. R.; Ouellette, W.; Korter, T. M. Investigation of (1R,2S)-(−)-ephedrine by cryogenic terahertz spectroscopy and solid-state density functional theory. *ChemPhysChem* **2009**, *10*, 2434−44.
(131) Allis, D. G.; Korter, T. M. Theoretical analysis of the terahertz spectrum of the high explosive PETN. *ChemPhysChem* **2006**, *7*, 2398−408.
(132) Jepsen, P. U.; Clark, S. J. Precise *ab-initio* prediction of terahertz vibrational modes in crystalline systems. *Chem. Phys. Lett.* **2007**, *442*, 275−280.
(133) Parrott, E. P. J.; Zeitler, J. A.; Friščić, T.; Pepper, M.; Jones, W.; Day, G. M.; Gladden, L. F. Testing the sensitivity of terahertz spectroscopy to changes in molecular and supramolecular structure: A study of structurally similar cocrystals. *Cryst. Growth Des.* **2009**, *9*, 1452−1460.
(134) Ayala, A. P. Polymorphism in drugs investigated by low wavenumber Raman scattering. *Vib. Spectrosc.* **2007**, *45*, 112−116.
(135) Korter, T. M.; Balu, R.; Campbell, M. B.; Beard, M. C.; Gregurick, S. K.; Heilweil, E. J. Terahertz spectroscopy of solid serine and cysteine. *Chem. Phys. Lett.* **2006**, *418*, 65−70.
(136) Dampf, S. J.; Korter, T. M. Anomalous temperature dependence of the lowest-frequency lattice vibration in crystalline γ-aminobutyric acid. *J. Phys. Chem. A* **2019**, *123*, 2058−2064.
(137) Allis, D. G.; Hakey, P. M.; Korter, T. M. Terahertz spectroscopy of illicit drugs: Experiment and theory. In *Frontiers in Optics 2008/Laser Science XXIV/Plasmonics and Metamaterials/Optical Fabrication and Testing*; OF&T, 2008; p LThB2.
(138) Lu, M.; Shen, J.; Li, N.; Zhang, Y.; Zhang, C.; Liang, L.; Xu, X. Detection and identification of illicit drugs using terahertz imaging. *J. Appl. Phys.* **2006**, *100*, 103104.
(139) Davies, A. G.; Burnett, A. D.; Fan, W.; Linfield, E. H.; Cunningham, J. E. Terahertz spectroscopy of explosives and drugs. *Mater. Today* **2008**, *11*, 18−26.
(140) Kawase, K.; Ogawa, Y.; Watanabe, Y.; Inoue, H. Non-destructive terahertz imaging of illicit drugs using spectral fingerprints. *Opt. Express* **2003**, *11*, 2549−2554.
(141) Shibata, T.; Mori, T.; Kojima, S. Low-frequency vibrational properties of crystalline and glassy indomethacin probed by terahertz time-domain spectroscopy and low-frequency Raman scattering. *Spectrochim. Acta, Part A* **2015**, *150*, 207−211.

https://doi.org/10.1021/acs.cgd.1c00850
Cryst. Growth Des. 2022, 22, 939−953

(142) Hédoux, A.; Paccou, L.; Guinet, Y.; Willart, J.-F.; Descamps, M. Using the low-frequency Raman spectroscopy to analyze the crystallization of amorphous indomethacin. *Eur. J. Pharm. Sci.* **2009**, *38*, 156−164.
(143) Berzins, K.; Sales, R. E.; Barnsley, J. E.; Walker, G.; Fraser-Miller, S. J.; Gordon, K. C. Low-wavenumber Raman spectral database of pharmaceutical excipients. *Vib. Spectrosc.* **2020**, *107*, 103021.
(144) Carriere, J. T.; Havermeyer, F.; Heyler, R. A. THz-Raman spectroscopy for explosives, chemical, and biological detection. In *Chemical, Biological, Radiological, Nuclear, and Explosives (CBRNE) Sensing XIV*; SPIE, 2013; p 87100M.
(145) Shi, L.; Duan, X.-H.; Zhu, L.-G.; Pei, C.-H. Low-temperature dependence on the THz spectrum of CL-20/TNT energetic cocrystal by molecular dynamics simulations. *J. Mol. Model.* **2020**, *26*, 25.
(146) Shen, Y. C.; Lo, T.; Taday, P. F.; Cole, B. E.; Tribe, W. R.; Kemp, M. C. Detection and identification of explosives using terahertz pulsed spectroscopic imaging. *Appl. Phys. Lett.* **2005**, *86*, 241116.
(147) Squires, A. D.; Kelly, M.; Lewis, R. A. Terahertz analysis of quinacridone pigments. *J. Infrared, Millimeter, Terahertz Waves* **2017**, *38*, 314−324.
(148) Squires, A. D.; Zaczek, A. J.; Lewis, R. A.; Korter, T. M. Identifying and explaining vibrational modes of quinacridones via temperature-resolved terahertz spectroscopy: Absorption experiments and solid-state density functional theory simulations. *Phys. Chem. Chem. Phys.* **2020**, *22*, 19672−19679.
(149) Ruggiero, M. T.; Sibik, J.; Zeitler, J. A.; Korter, T. M. Examination of l-glutamic acid polymorphs by solid-state density functional theory and terahertz spectroscopy. *J. Phys. Chem. A* **2016**, *120*, 7490−7495.
(150) Ruggiero, M. T.; Sutton, J. J.; Fraser-Miller, S. J.; Zaczek, A. J.; Korter, T. M.; Gordon, K. C.; Zeitler, J. A. Revisiting the thermodynamic stability of indomethacin polymorphs with low-frequency vibrational spectroscopy and quantum mechanical simulations. *Cryst. Growth Des.* **2018**, *18*, 6513−6520.
(151) Davis, M. P.; Mohara, M.; Shimura, K.; Korter, T. M. Simulation and assignment of the terahertz vibrational spectra of enalapril maleate cocrystal polymorphs. *J. Phys. Chem. A* **2020**, *124*, 9793−9800.
(152) Delaney, S. P.; Smith, T. M.; Korter, T. M. Conformation versus cohesion in the relative stabilities of gabapentin polymorphs. *RSC Adv.* **2014**, *4*, 855−864.
(153) Rexrode, N. R.; Orien, J.; King, M. D. Effects of solvent stabilization on pharmaceutical crystallization: Investigating conformational polymorphism of probucol using combined solid-state density functional theory, molecular dynamics, and terahertz spectroscopy. *J. Phys. Chem. A* **2019**, *123*, 6937−6947.
(154) Heinz, A.; Strachan, C. J.; Gordon, K. C.; Rades, T. Analysis of solid-state transformations of pharmaceutical compounds using vibrational spectroscopy. *J. Pharm. Pharmacol.* **2010**, *61*, 971−988.
(155) Robert, C.; Fraser-Miller, S. J.; Berzins, K.; Okeyo, P. O.; Rantanen, J.; Rades, T.; Gordon, K. C. Monitoring the isothermal dehydration of crystalline hydrates using low-frequency Raman spectroscopy. *Mol. Pharmaceutics* **2021**, *18*, 1264−1276.
(156) Salzillo, T.; Della Valle, R. G.; Venuti, E.; Brillante, A.; Siegrist, T.; Masino, M.; Mezzadri, F.; Girlando, A. Two new polymorphs of the organic semiconductor 9, 10-diphenylanthracene: Raman and x-ray analysis. *J. Phys. Chem. C* **2016**, *120*, 1831−1840.
(157) Kissi, E. O.; Grohganz, H.; Löbmann, K.; Ruggiero, M. T.; Zeitler, J. A.; Rades, T. Glass-transition temperature of the β-relaxation as the major predictive parameter for recrystallization of neat amorphous drugs. *J. Phys. Chem. B* **2018**, *122*, 2803−2808.
(158) Suzuki, H.; Hoshina, H.; Otani, C. Kinetics of polymorphic transitions of cyclohexanol investigated by terahertz absorption spectroscopy. *Cryst. Growth Des.* **2014**, *14*, 4087−4093.
(159) Ruggiero, M. T.; Axel Zeitler, J.; Korter, T. M. Concomitant polymorphism and the martensitic-like transformation of an organic crystal. *Phys. Chem. Chem. Phys.* **2017**, *19*, 28502−28506.
(160) Delaney, S. P.; Pan, D.; Galella, M.; Yin, S. X.; Korter, T. M. Understanding the origins of conformational disorder in the crystalline polymorphs of irbesartan. *Cryst. Growth Des.* **2012**, *12*, 5017−5024.
(161) King, M. D.; Blanton, T. N.; Misture, S. T.; Korter, T. M. Prediction of the unknown crystal structure of creatine using fully quantum mechanical methods. *Cryst. Growth Des.* **2011**, *11*, 5733−5740.
(162) McIntosh, A. I.; Yang, B.; Goldup, S. M.; Watkinson, M.; Donnan, R. S. Crystallization of amorphous lactose at high humidity studied by terahertz time domain spectroscopy. *Chem. Phys. Lett.* **2013**, *558*, 104−108.
(163) Liu, H.-B.; Zhang, X.-C. Dehydration kinetics of d-glucose monohydrate studied using THz time-domain spectroscopy. *Chem. Phys. Lett.* **2006**, *429*, 229−233.
(164) Sibik, J.; Sargent, M. J.; Franklin, M.; Zeitler, J. A. Crystallization and phase changes in paracetamol from the amorphous solid to the liquid phase. *Mol. Pharmaceutics* **2014**, *11*, 1326−1334.
(165) Inoue, M.; Hisada, H.; Koide, T.; Carriere, J.; Heyler, R.; Fukami, T. In situ monitoring of crystalline transformation of carbamazepine using probe-type low-frequency Raman spectroscopy. *Org. Process Res. Dev.* **2017**, *21*, 262−265.
(166) Sibik, J.; Löbmann, K.; Rades, T.; Zeitler, J. A. Predicting crystallization of amorphous drugs with terahertz spectroscopy. *Mol. Pharmaceutics* **2015**, *12*, 3062−3068.
(167) Ge, M.; Wang, W.; Zhao, H.; Zhang, Z.; Yu, X.; Li, W. Characterization of crystal transformation in the solid-state by terahertz time-domain spectroscopy. *Chem. Phys. Lett.* **2007**, *444*, 355−358.
(168) Inoue, M.; Hisada, H.; Koide, T.; Carriere, J.; Heyler, R.; Fukami, T. Real-time formation monitoring of cocrystals with different stoichiometries using probe-type low-frequency Raman spectroscopy. *Ind. Eng. Chem. Res.* **2017**, *56*, 12693−12697.
(169) Otaki, T.; Tanabe, Y.; Kojima, T.; Miura, M.; Ikeda, Y.; Koide, T.; Fukami, T. In situ monitoring of cocrystals in formulation development using low-frequency Raman spectroscopy. *Int. J. Pharm.* **2018**, *542*, 56−65.
(170) Liu, X.; Liu, G.; Zhao, H.; Zhang, Z.; Wei, Y.; Liu, M.; Wen, W.; Zhou, X. The quantitative monitoring of mechanochemical reaction between solid l-tartaric acid and sodium carbonate monohydrate by terahertz spectroscopy. *J. Phys. Chem. Solids* **2011**, *72*, 1245−1250.
(171) Lien Nguyen, K.; Friščić, T.; Day, G. M.; Gladden, L. F.; Jones, W. Terahertz time-domain spectroscopy and the quantitative monitoring of mechanochemical cocrystal formation. *Nat. Mater.* **2007**, *6*, 206−209.
(172) Zhou, J.; Xu, H.; Shi, Y.; Li, J. Terahertz driven reversible topological phase transition of monolayer transition metal dichalcogenides. *Adv. Sci.* **2021**, *8*, 2003832.
(173) Ruggiero, M. T.; Krynski, M.; Kissi, E. O.; Sibik, J.; Markl, D.; Tan, N. Y.; Arslanov, D.; van der Zande, W.; Redlich, B.; Korter, T. M.; Grohganz, H.; Löbmann, K.; Rades, T.; Elliott, S. R.; Zeitler, J. A. The significance of the amorphous potential energy landscape for dictating glassy dynamics and driving solid-state crystallisation. *Phys. Chem. Chem. Phys.* **2017**, *19*, 30039−30047.
(174) Greaves, G. N. Identifying vibrations that destabilize crystals and characterize the glassy state. *Science* **2005**, *308*, 1299−1302.
(175) Damari, R.; Weinberg, O.; Krotkov, D.; Demina, N.; Akulov, K.; Golombek, A.; Schwartz, T.; Fleischer, S. Strong coupling of collective intermolecular vibrations in organic materials at terahertz frequencies. *Nat. Commun.* **2019**, *10*, 3248.
(176) Burtch, N. C.; Heinen, J.; Bennett, T. D.; Dubbeldam, D.; Allendorf, M. D. Mechanical properties in metal−organic frameworks: emerging opportunities and challenges for device functionality and technological applications. *Adv. Mater.* **2018**, *30*, 1704124.
(177) Erba, A.; Mahmoud, A.; Belmonte, D.; Dovesi, R. High pressure elastic properties of minerals from ab initio simulations: The case of pyrope, grossular and andradite silicate garnets. *J. Chem. Phys.* **2014**, *140*, 124703.

https://doi.org/10.1021/acs.cgd.1c00850
Cryst. Growth Des. 2022, 22, 939−953

(178) Erba, A.; Ruggiero, M. T.; Korter, T. M.; Dovesi, R. Piezo-optic tensor of crystals from quantum-mechanical calculations. *J. Chem. Phys.* **2015**, *143*, 144504.
(179) Erba, A.; Dovesi, R. Photoelasticity of crystals from theoretical simulations. *Phys. Rev. B: Condens. Matter Mater. Phys.* **2013**, *88*, 045121.
(180) Perger, W.; Criswell, J.; Civalleri, B.; Dovesi, R. Ab-initio calculation of elastic constants of crystalline systems with the CRYSTAL code. *Comput. Phys. Commun.* **2009**, *180*, 1753−1759.
(181) Ortiz, A. U.; Boutin, A.; Fuchs, A. H.; Coudert, F.-X. Investigating the pressure-induced amorphization of zeolitic imidazolate framework ZIF-8: Mechanical instability due to shear mode softening. *J. Phys. Chem. Lett.* **2013**, *4*, 1861−1865.
(182) Elder, R. M.; Zaccone, A.; Sirk, T. W. Identifying nonaffine softening modes in glassy polymer networks: A pathway to chemical design. *ACS Macro Lett.* **2019**, *8*, 1160−1165.
(183) Ryder, M. R.; Civalleri, B.; Tan, J.-C. Isoreticular zirconium-based metal−organic frameworks: discovering mechanical trends and elastic anomalies controlling chemical structure stability. *Phys. Chem. Chem. Phys.* **2016**, *18*, 9079−9087.
(184) Nguyen-Thanh, T.; Bosak, A.; Bauer, J. D.; Luchitskaia, R.; Refson, K.; Milman, V.; Winkler, B. Lattice dynamics and elasticity of $SrCO_3$. *J. Appl. Crystallogr.* **2016**, *49*, 1982−1990.
(185) Ryder, M. R.; Civalleri, B.; Bennett, T. D.; Henke, S.; Rudić, S.; Cinque, G.; Fernandez-Alonso, F.; Tan, J.-C. Identifying the role of terahertz vibrations in metal-organic frameworks: From gate-opening phenomenon to shear-driven structural destabilization. *Phys. Rev. Lett.* **2014**, *113*, 215502.
(186) Maul, J.; Ryder, M. R.; Ruggiero, M. T.; Erba, A. Pressure-driven mechanical anisotropy and destabilization in zeolitic imidazolate frameworks. *Phys. Rev. B: Condens. Matter Mater. Phys.* **2019**, *99*, 014102.
(187) Erba, A.; Maul, J.; Demichelis, R.; Dovesi, R. Assessing thermochemical properties of materials through ab initio quantum-mechanical methods: the case of α-Al_2O_3. *Phys. Chem. Chem. Phys.* **2015**, *17*, 11670−11677.
(188) Goodwin, A. L.; Kepert, C. J. Negative thermal expansion and low-frequency modes in cyanide-bridged framework materials. *Phys. Rev. B: Condens. Matter Mater. Phys.* **2005**, *71*, 140301R.
(189) Ryder, M. R.; Bennett, T. D.; Kelley, C. S.; Frogley, M. D.; Cinque, G.; Tan, J.-C. Tracking thermal-induced amorphization of a zeolitic imidazolate framework via synchrotron in situ far-infrared spectroscopy. *Chem. Commun.* **2017**, *53*, 7041−7044.
(190) Barron, T.; Collins, J.; White, G. Thermal expansion of solids at low temperatures. *Adv. Phys.* **1980**, *29*, 609−730.
(191) Zhang, Y.; Manke, D. R.; Sharifzadeh, S.; Briseno, A. L.; Ramasubramaniam, A.; Koski, K. J. The elastic constants of rubrene determined by Brillouin scattering and density functional theory. *Appl. Phys. Lett.* **2017**, *110*, 071903.

https://doi.org/10.1021/acs.cgd.1c00850
Cryst. Growth Des. 2022, 22, 939−953